

Award Accounts

The Chemical Society of Japan Award for Creative Work for 2004

Chemical Biology that Controls DNA Structure and Function: Lessons in Organic Chemistry from Nature

Hiroshi Sugiyama

Department of Chemistry, Graduate School of Science, Kyoto University, Kitashirakawa-Oiwakecho, Sakyo-ku, Kyoto 606-8502

Received August 1, 2006; E-mail: hs@kuchem.kyoto-u.ac.jp

Fifty years after the discovery of the double-helical structure of DNA, the complete sequence of the human genome has been determined. All genetic information, which is necessary for life, is written in 30 billion base pairs of DNA. Many diseases, including cancer, and hereditary and viral diseases, can now be understood at the DNA sequence level. Local DNA conformations are also thought to play an important role in biological processes, such as gene expression. Therefore, DNA sequences and local DNA conformations are the targets of novel drugs that would precisely switch certain genes on or off. Modified bases that perform various functions can also be incorporated into defined DNA sequences. DNA can now be synthesized by the phosphoramidite method and amplified by PCR, and by using organisms such as *Escherichia coli*, DNA becomes a promising unit for nanotechnology applications. In this review, I focus on our efforts in understanding the DNA reactivity, structure, and function of DNA. The prospective uses of the chemical biology of DNA will also be discussed.

Chemistry has greatly contributed to the understanding of cellular processes by allowing the identification of metabolic pathways, enzymatic processes, and signal transduction mechanisms. Understanding of the chemistry of nucleic acids has played a key role in the progressive development of molecular biology and life science through the development of many epoch-making techniques, such as the DNA sequencing, the synthesis of oligonucleotides, and PCR amplification. During my Ph.D. course, I started research on photochemistry between DNA and proteins as a model of photoinduced DNA–protein crosslinking for examining the ternary structure of the nucleosome and understanding the mechanisms of photodamage of DNA. We found that the ε-amino group of the lysine residues of histone crosslinked with thymine residues in DNA.[1] Interestingly, the crosslink site was cleaved upon heating to regenerate the thymine ring on the ε-amino group of the lysine residues in the protein by Michael addition (Figure 1). At that time, not so many researchers were interested in chemical modification in a nucleosome.

Because we applied this photoreaction for T specific cleavage of DNA,[1d] I was attracted to the molecular mechanisms of DNA modification at an atomic level. I had the chance to study the mechanism of action of the antitumor antibiotic bleomycin at Sidney Hecht's group at the University of Virginia from 1984 to 1986. We investigated how these glycopeptides recognize specific DNA sequences and efficiently oxidize C4′ deoxyribose to induce DNA strand cleavage using synthetic oligonucleotides with defined sequences.[2] We identified the formation of C4′ hydroxy abasic sites in addition to the known oxidative direct-strand scission via a Criegee type rearrangement of the C4′ hydroperoxy intermediate.[3] We found that the C4′ hydroxy abasic site generated by Fe-bleomycin underwent aldol condensation and subsequent elimination and rearrangement to produce cyclic hydroxy pentenone termini.

After returning to Kyoto University, I studied the mechanisms of DNA strand cleavage by various antitumor antibiotics such as bleomycin,[4] neocarzinostatin,[5] kapurimycin A3,[6] duocarmycin A (Duo),[7] and carzinophilin.[8] Using oligonucleotides, we identified well-programmed and specific reactions with DNA by these natural products. As shown in Fig. 2, these antibiotics carry out beautiful atom-specific reactions on superficially monotonous double-stranded DNA. Kapurimycin A3, Duo, and carzinophiline are antitumor antibiotics produced by Streptomyces. Kapurimycin A3 and Duo have epoxide or cyclopropane as their respective active sites, which produce covalent bonds with DNA at purine N9 and N3, respectively. Carzinophilin has aziridine and epoxide moieties. We demonstrated cooperative alkylation at the aziridine moiety with the adenine N7 and subsequent crosslinking of the epoxide moiety and the guanine N7 position. We found that C4′ hydroxy abasic sites efficiently formed in DNA by Co–BLM complex under UV irradiation conditions.[4a] Forming C4′ radical by Fe– and Co–BLM was firstly detected using radical clock.[4c] In the neocarzinostatin reaction, we found competitive C4′ and C5′ hydrogen abstraction at the GT step by thiol-activated neocarzinostatin. These results clearly indicated that a carbon radi-

Published on the web May 14, 2007; doi:10.1246/bcsj.80.823

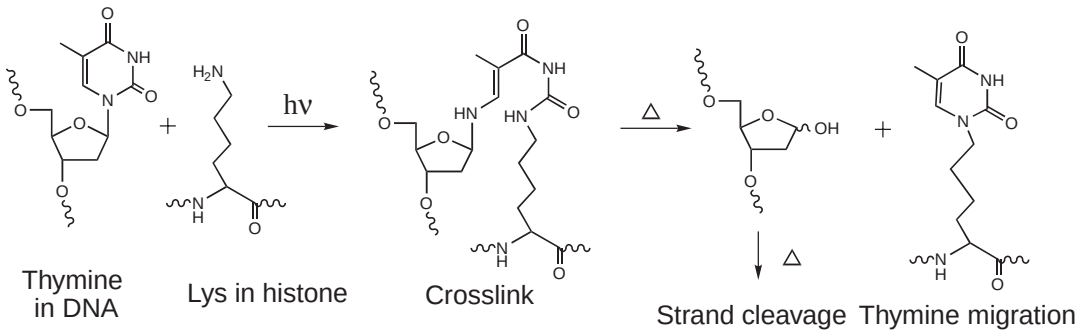

Fig. 1. Photocrosslink between lysine in histone and thymine in DNA and subsequent migration of thymine and DNA strand cleavage.

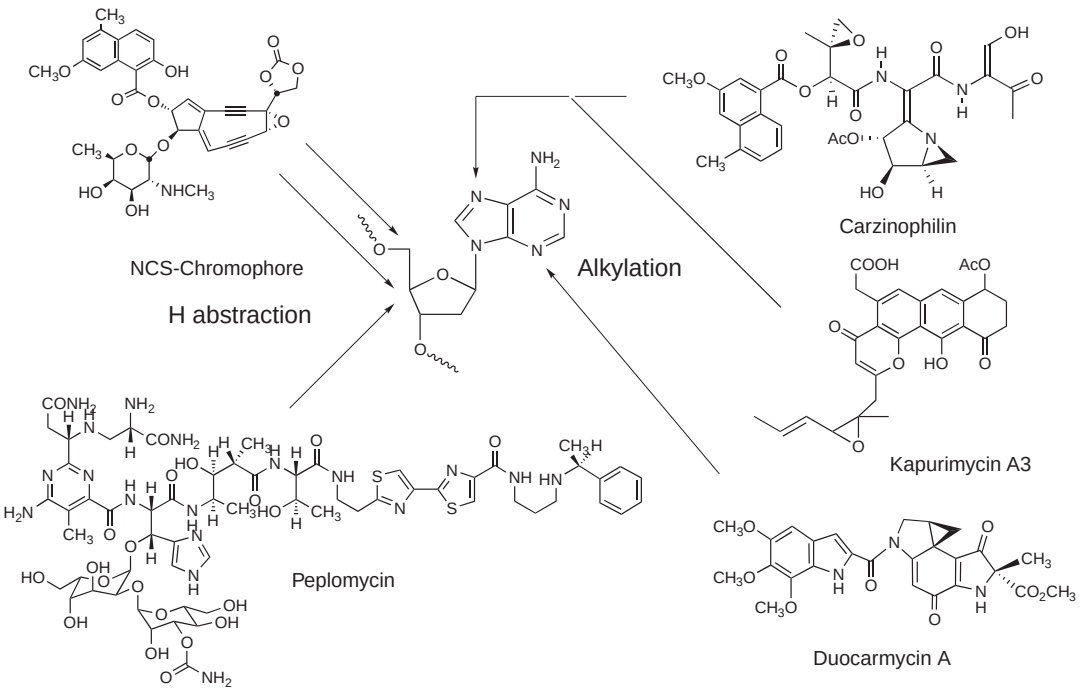

Fig. 2. Chemical structures of antitumor antibiotics and their sites of atom specific modification.

cal might be located in proximity to C4′ and C5′ hydrogens.[5c] Based on this reactivity, we proposed a binding model of the DNA–neocarzinostatin complex that is in good agreement with the NMR structure of a subsequently reported complex.[9]

The reactivity of antitumor antibiotics is just like that occurring in a primitive version of an enzyme. Even highly skilled synthetic organic chemists cannot design DNA-modifying agents from scratch. Therefore, we need to learn more about molecular recognition from natural products that act on DNA, such as how to read sequences, the reaction mechanisms, and how to achieve efficient and specific reactions. Because the photocrosslinking reaction of thymine with lysine requires specific pairs in certain proximity and only proceeds under basic conditions, it is not a general reaction used to probe DNA–protein interactions. Therefore, we decided to use 5-halouracil to examine DNA–protein interactions. However, we found that photocrosslinks between 5-halouracil-containing DNA and protein were not always useful in obtaining new general knowledge of DNA–protein interactions. Interestingly, we found that hydrogen abstraction in DNA by the uracil-5-yl radical generated from the 5-halouracil residue under UV irradiation was atom-specific and highly dependent on DNA structure. This photochemical method, which reflects DNA structure, could be applied as a unique conformational probe of DNA in living cells. Moreover, it was revealed that the photoreactivities of 5-halouracil-containing DNA could be used to monitor electron-transfer processes that are substantially influenced by DNA structure. In this account, our recent progress in the investigation of the chemical biology of DNA is summarized.

1. Recognition of DNA Sequences

About ten years ago, we discovered that the addition of distamycin A (Dist) dramatically changes alkylation sites, primarily at the G residues in GC-rich sequences, by forming a cooperative heterodimer between Duo and Dist.[10] The NMR refined structure of a Duo–Dist–d(CAGGTGGT)/d(ACCACCTG) complex demonstrated that heterodimers of Duo and Dist tightly bound to the minor groove of DNA duplexes. Importantly, the replacement of Dist with various Py–Im tri-

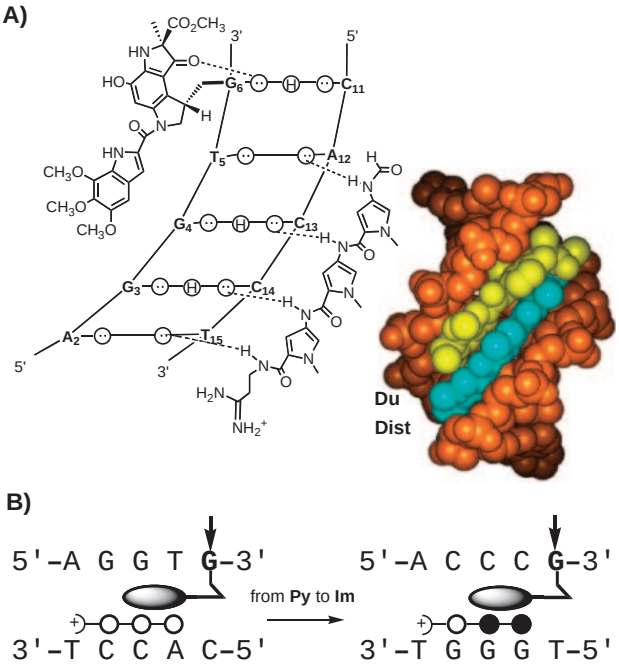

Fig. 3. CPK model of NMR refined structure of Duodistamycin A-DNA complex (A) and schematic presentation of their molecular recognition (B).

amides changed the sequence-specific alkylation by Duo in a predictive manner,[11] with two N-terminal Py units of Dist recognizing the complementary strand of the reacting octamer according to the base-pair recognition rule of Py–Im polyamides in the minor groove (Fig. 3).

1.1 Design of Sequence-Specific DNA Alkylating Agent. The above findings suggest that Py–Im polyamides can be used as versatile sequence-recognition components of sequence-specific DNA-alkylating conjugates. Py–Im hairpin polyamides with a γ-aminobutyric acid turn were demonstrated to be useful DNA-binding units, with both increased specificity and affinity, as confirmed by NMR spectroscopy.[12] Thus, we linked alkylating Py–Im polyamides and partner polyamides with a g-aminobutyric acid linker to make **1** and **2**. Conjugate **1** mainly alkylated the A of the 5′-TGTAA**A**-3′ sequence within several hundred bp DNA fragments. Similarly, alkylation by conjugate **2** occurred at targeted sequences, such as the G of 5′-AGTCA**G**-3′, at nanomolar concentrations (Fig. 4).[13] Independently, other groups have also synthesized different types of alkylating Py–Im polyamides.[14]

Although highly specific alkylation was achieved by **1** and **2** in these systems, alkylation is rather slow; the efficiency of DNA alkylation by **1** and **2** was 1.6 and 7.4%, respectively. Molecular dynamics simulation of a **1**–octamer complex suggested that the position of cyclopropane is between two bases, which explains the low efficiency of the reactions by **1** and **2**. It was also suggested that the insertion of a vinyl linker (L) between the Py–Im polyamide and alkylating moiety of Duo would change the location of the cyclopropane ring and improve the DNA-alkylating efficacy of the conjugates. Thus, we synthesized Py–Im diamide conjugates with a vinyl linker. Due to the low coupling yield of alkylating moiety of Duo with the PyIm dimer with acrylic acid, we required more rigorous

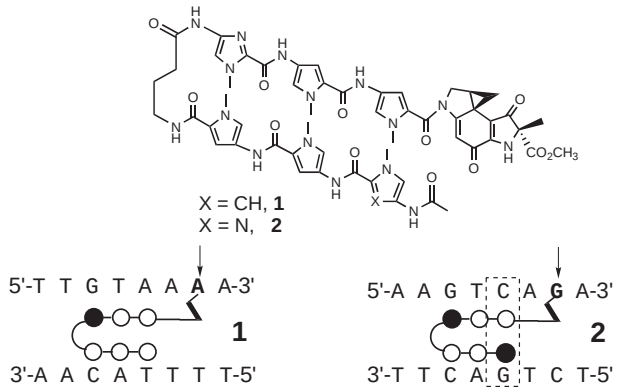

Fig. 4. Chemical structures of the conjugates **1** and **2**, and a schematic presentation of the specific alkylation by **1** and **2**. Im is indicated by the black circles, and Py the open circles. ⊂ represents the γ-aminobutanoic acid turn residue connecting the two subunits.

coupling conditions. We, therefore, introduced cyclopropylindole (CPI), which is more stable than alkylating moiety of Duo. The DNA-alkylating CPI moiety can be prepared in five steps from the antibiotic duocarmycin B_2 with an overall 25% yield.[15] Thus, we synthesized ImPyLCPI (**3**) and found that **3** caused DNA alkylation of the 5′-PyG(A/T)C**Pu**-3′ sequence with highly efficiently. Quantitative sequencing analysis using top and bottom strand labeled DNA fragments indicated that alkylation occurred through highly cooperative homodimer formation.[16] We found that the efficiency of alkylation by **3** was 69%, thus confirming the surprisingly high efficiency of dialkylation compared to the Py–Im alkylating polyamides without a vinyl linker (Fig. 5). Analogously, Py–Im triamide conjugates **4** and **5** sequence-specifically alkylate the target sequences in supercoiled plasmid DNA such as pQBI PGK (5387 bp), which then has inhibitory effects on DNA hydrolysis by restricting endonucleases *Bss*H II and *Eco*52 I (Fig. 5).[17] These results clearly demonstrate that **4** and **5** selectively alkylate DNA at matching sequences, even within several thousand base pairs of supercoiled DNA. These results also indicated that DNA alkylation in the minor groove by Py–Im polyamides strongly affected DNA–protein interactions.

1.2 Design of Sequence-Specific DNA Interstrand Crosslinking Agent. The observation of highly efficient DNA alkylation by polyamides with vinyl linkers encouraged us to synthesize dimer molecules of **3** to develop DNA interstrand crosslinking agents with sequence specificity. As DNA interstrand crosslinking agents directly inhibit both DNA replication and gene expression by preventing the melting of DNA strands, crosslinking agents are expected to have potent antitumor activity.[18] We synthesized several dimers of ImPyLCPI **3**, and developed a novel DNA interstrand crosslinking agent **6** with a tetramethylene linker. It was revealed that compound **6** crosslinked double stranded DNA at the nine-base-pair sequence 5′-PyGGC(T/A)GCC**Pu**-3′, but only in the presence of the triamide ImImPy (Fig. 6).[19] The present system consisted of a 1:2 heterodimer complex of the alkylating agent and partner ImImPy in the DNA minor groove and caused interstrand crosslinking in a sequence-specific fashion according to the base-pair recognition rule of Py–Im polyamides.

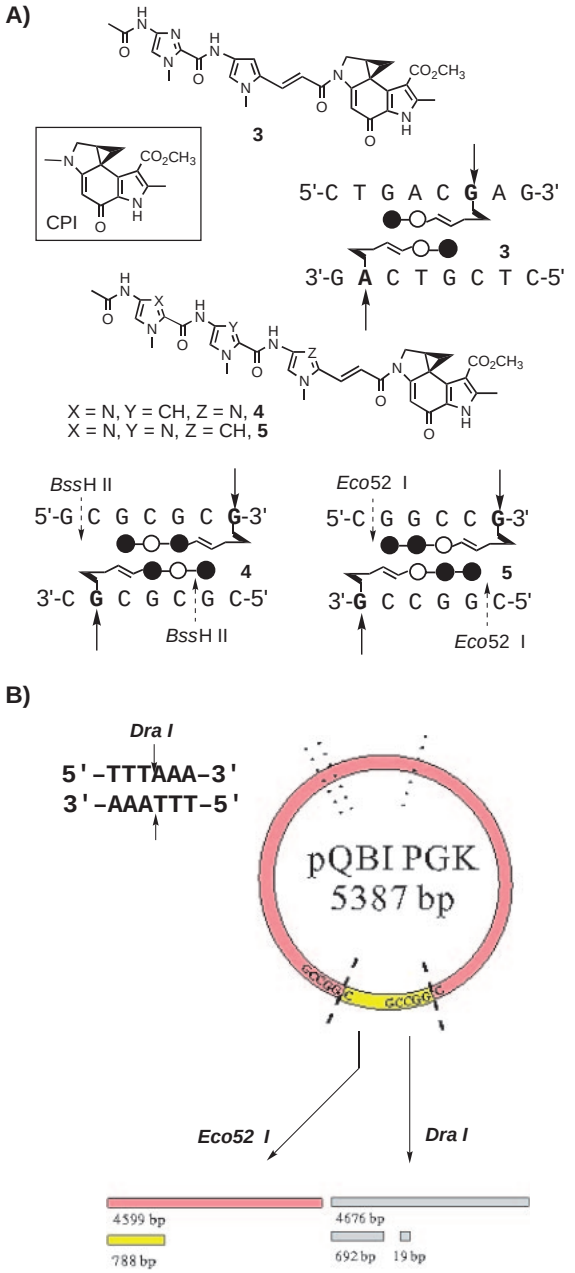

Fig. 5. (A) Chemical structures of CPI conjugates **3**–**5**, and a schematic presentation of the specific alkylation by **3**–**5** through homodimer formation and a selective inhibition of Eco52 I hydrolysis of pQBIPGK plasmid by **5** (B). Dotted arrows indicate the site of hydrolysis by restriction endonucleases.

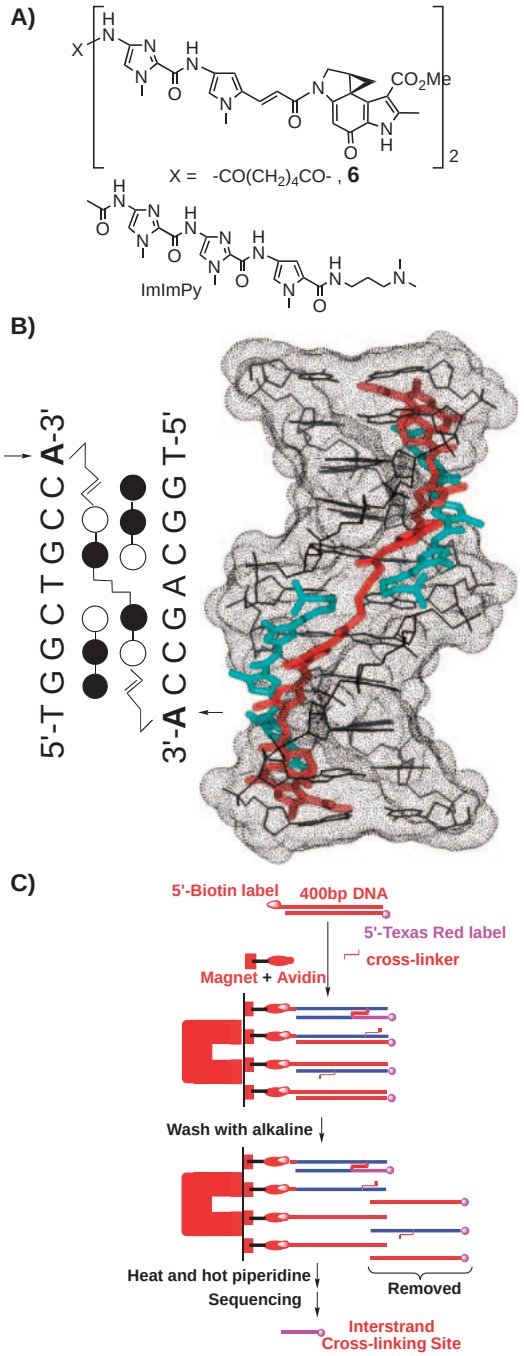

Fig. 6. (A) Chemical structures of interstrand crosslinker **6** and ImImPy. (B) Schematic presentation of the sequence-specific interstrand crosslining by **6** in the presence of ImImPy (left). The energy-minimized model of the d(TGGCTGCCA)/d(TGGCAGCCA)-**6**-ImImPy complex (right). (C) Schematic presentation of identification of site of interstrand crosslink using biotin-labeled DNA.

To demonstrate that such interstrand crosslinks occur in longer DNA fragments, we developed a new method using a double-labeled DNA fragment system with one strand biotin-labeled and the other labeled with Texas Red (Fig. 6C). After DNA alkylation, DNA fragments were separated using streptavidin bound to magnetic beads and washed with an alkaline solution. Under such conditions, the Texas Red-labeled fragments obtained should only be those crosslinked to the biotin-labeled fragment. Densitometric analysis indicated that the contribution of interstrand crosslinking to the observed alkylation bands was approximately 40%. This compound efficiently crosslinked both strands at the target sequence.[19b] The system consisted of a 1:2 complex of the alkylating agent and its partner ImImPy, and interstrand crosslinking occurred in a sequence-specific fashion according to the base-pair recognition rule of Py–Im polyamides.

1.3 Design of Sequence-Specific DNA Alkylating Hairpin Polyamide. Since insertion of a L between the Py–Im polyamides and CPI dramatically enhanced DNA-alkylating reactivity, we synthesized CPI and Py–Im polyamide hairpin conjugates **7**–**10** with vinyl linkers.[20] Sequencing gel analysis indicated that conjugates **7**–**10** with vinyl linkers effectively alkylated DNA at the N3 position of both adenines and guanines in each matching sequence in DNA fragment. DNA alkylation was basically complete within 5 min at nanomolar concentrations. This was in clear contrast to the fact that hairpin polyamides without vinyl linkers did not cause alkylation even after 1 h of incubation.[13] The observation of efficient sequence-specific alkylation by conjugates **7**–**10** (Fig. 7) encouraged us to examine further the biological activity induced by specific DNA alkylation with these agents.

1.4 Improvement of the Alkylating Moiety of Hairpin Polyamide. Although the insertion of L between CPI and the Py–Im polyamides dramatically enhanced the DNA-alkylating activity by more than 100-fold compared to that without L,[19] it was not practical for us to synthesize sufficient quantities of Py–Im CPI conjugates for animal studies. To overcome this problem, we searched for an alternative alkylating moiety that is equivalent to CPI in terms of its DNA alkylation and that could be synthesized from commercially available starting materials using a general synthetic methodology. Boger and colleagues have demonstrated that 1,2,9,9a-tetrahydrocyclopropa[1,2-*c*]benz[1,2-*e*]indol-4-one (CBI) is more stable than CPI in aqueous solution and that DNA-alkylating conjugates with high stability at neutral pH have a higher cytotoxicity.[21] Therefore, we selected CBI as the DNA-alkylating unit and synthesized hairpin polyamides possessing both enantiomers of CBI, **11S** and **11R**. High-resolution denaturing gel electrophoresis indicated that **11S** efficiently alkylated the target sequence 5′-TGACCA-3′ in DNA fragments. The specificity and efficiency of DNA alkylation by **11S** were comparable to or even higher than those of the corresponding CPI conjugate **11**.[22] In contrast, enantiomer **11R** with an unnatural orientation of the cyclopropane ring showed very weak DNA-alkylating activity. Molecular modeling suggested that the different binding orientations of the *S*- and *R*-CBI units explained well the significant enantioselective reactivities of **11S** and **11R**.

Interestingly, despite having similar DNA-binding orientations, DNA alkylation CPI conjugate **7** occurred equally at N3 of both the A and G of the matching sequence, whereas CBI conjugate **11S** specifically alkylated only N3 of the A.[23] Importantly, it was also observed that CBI conjugates reduced the alkylation of mismatch sites. These results indicated that lowering the reactivity increased the base and sequence specificity, and the introduction of CBI further improved specificity to target sequences (Fig. 8).

1.5 Improvement of the Linker Region of Hairpin Polyamide. The L moiety has certain disadvantages in the synthesis of alkylating Py–Im polyamides, because it is relatively unstable under acidic and basic conditions and it suffers from low chemical yields. Since ethyl 3-(4-amino-*N*-methylpyrrol-2-yl)-acrylate is extremely unstable, solid-phase synthesis of Py–Im polyamides with vinyl linkers was not successful. Therefore, we synthesized various alkylating Py–Im polyamides by a combination of time-consuming liquid-phase coupling reactions.[13,16,17,19,24] To overcome these problems, we searched for a new linker that is stable and could provide the same geometry as Py with L. A 5-amino-1*H*-indole-2-carbonyl linker (indole linker) was used as the new linker, because the amide linkages of this unit were approximately superimposable with Py with a vinyl linker, which was supported by molecular orbital calculations at the B3LYP/6-31G* level. Thus, CBI conjugates **12**, **13**, and seco-CBI conjugate **14** with an indole linker were synthesized by a combination of Fmoc solid-phase synthesis using an oxime resin[25] and a subsequent liquid-phase coupling procedure. Conjugates **12**, **13**, and **14** efficiently alkylate the specific sequences, 5′-WWWCC**A**-3′ and 5′-

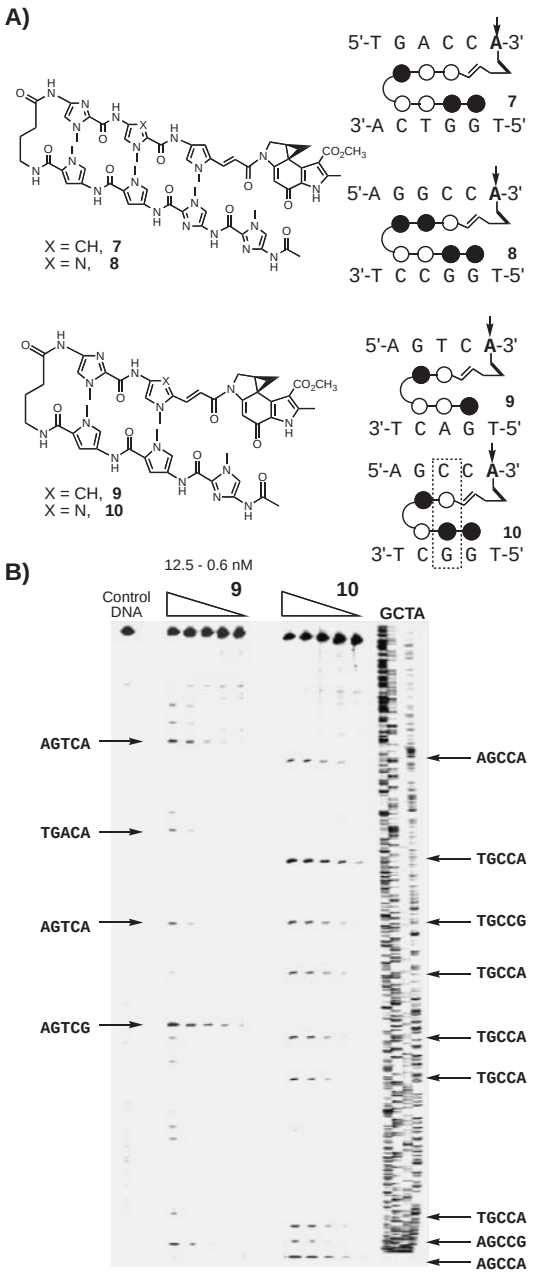

Fig. 7. (A) Chemical structures and a schematic presentation of the specific alkylation of Py–Im hairpin conjugates **7**–**10** and (B) thermally induced sequence-specific strand cleavage by **9** and **10**.

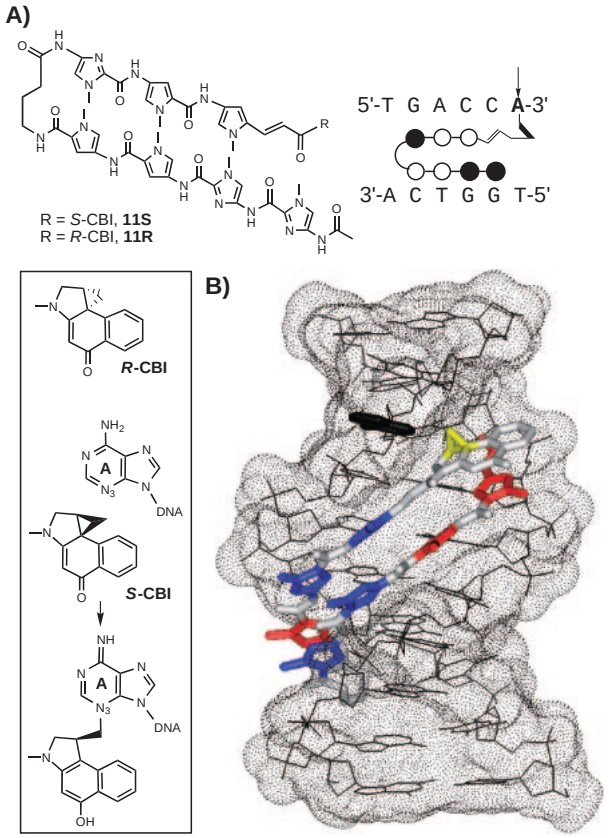

Fig. 8. (A) Chemical structures of **11S** and **11R** and a schematic presentation of specific alkylation by Py–Im hairpin conjugate **11S**. (B) The energy-minimized model of the d(CTTGACCATG)/d(CATGGTCAAG)-**11S** complex.

WGWCC**A**-3′ (W = A or T). These results indicated that the indole linker was as an appropriate substitute for L. In particular, seco-CBI conjugate **15** alkylates a specific nine-base-pair sequence, 5′-ACAAATCC**A**-3′ (Fig. 9).[26] Introduction of an indole linker greatly facilitated the synthesis of sequence-specific alkylating Py–Im polyamides by effective use of solid phase Py–Im polyamide synthesis.

1.6 Gene Silencing by Sequence-Specific Alkylation by Py–Im Polyamide Conjugates. The control of specific gene expression by synthetic small molecules has emerged as a promising approach for gene-targeting drugs. We have recently shown that Py–Im polyamide **9**, which alkylates a specific site on the template strand of the coding region of green fluorescent protein (GFP), effectively inhibited transcription by alkylation, producing truncated mRNAs in an in vitro transcription system.[27] In sharp contrast, alkylation in the nontemplate strand did not give such truncated products. The inhibition of transcription by deactivated conjugate **16** was not observed by PAGE analysis, which confirmed that noncovalent binding does not cause inhibition of transcription (Fig. 10).

Sequence-specific gene silencing by the alkylating Py–Im conjugates **7** and **8**, which target the coding regions of renilla and firefly luciferases, respectively, was investigated. Two vector plasmids were transfected into HeLa cells, and their ability to silence luciferase expression was examined in vitro[28] (Fig. 11). Selective reduction of luciferase activities occurred

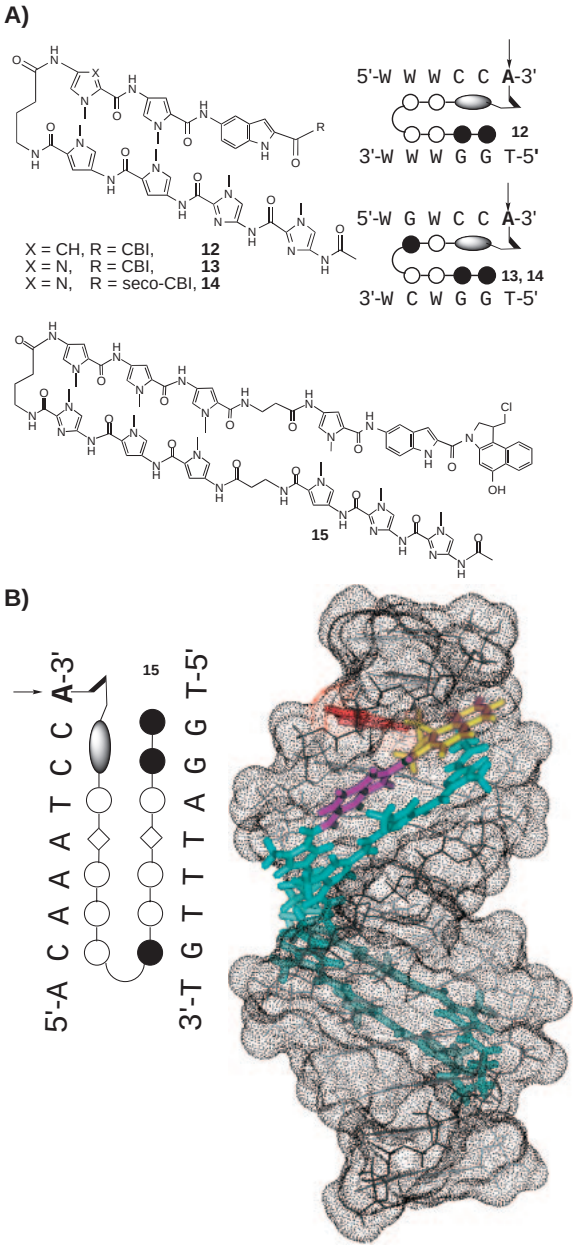

Fig. 9. (A) Chemical structures and a schematic presentation of specific alkylation by Py–Im hairpin conjugates **12–15** and (B) an energy-minimized model of the d(ATACAAATCCAAT)/d(ATTGGATTTGTAT)-**15** complex.

using caused by both polyamides. Based on this sequence-specific alkylation and gene silencing activity, these alkylating Py–Im polyamides thus have potential as antitumor drugs to target specific gene expression in human cells.

1.7 Selective Cytotoxicity of Sequence-Specific Alkylation by Py–Im Polyamide Conjugates. DNA-alkylating agents, such as the nitrosoureas, mitomycin C, and cisplatin, which constitute a major class of antitumor drugs, have long been of interest for their biological properties and are routinely used for cancer therapy. These drugs are usually very toxic to normal cells. One important question to be addressed is whether the introduction of sequence selectivity to an alkylating agent can improve its efficacy as an anticancer agent. In addi-

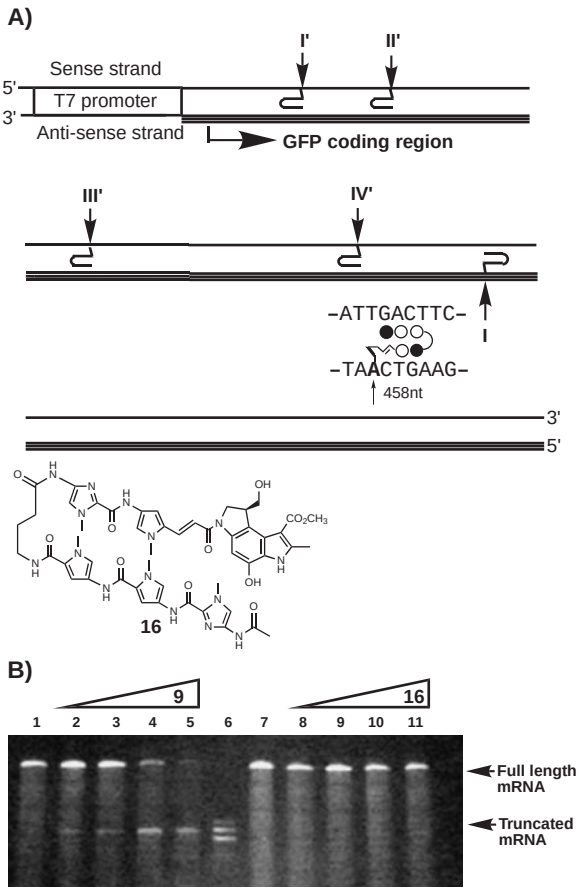

Fig. 10. The inhibition of GFP mRNA expression by sequence-specific alkylation at 5′-AGTCA-3′ by conjugate **9**. (A) A schematic presentation of the sites of alkylation in the GFP gene under the control of the T7 promoter. (B) PAGE analysis of transcripts of **9** or **16** treated DNA. The three bands in lane 7 are RNA markers.

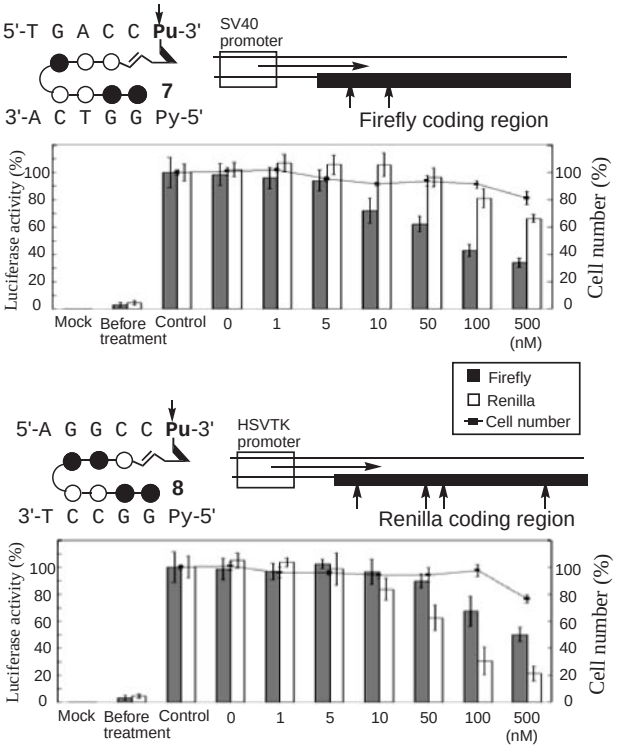

Fig. 11. A schematic presentation of the sites of alkylation in firefly and renilla luciferase vectors and selective inhibition of luciferase translation by sequence-specific alkylation with conjugates **7** and **8**.

tion, the question arises as to whether one can tailor the binding preference of DNA-binding agents to particular sequences to create thereby a tailor-made antitumor agent.

The progress in our study of DNA alkylation has led to methodology for the development of novel antitumor agents with sequence recognition ability, and DNA sequence specificity is one important component contributing to the cytotoxic potency of several alkylating Py–Im polyamides. We examined in detail comparative studies of DNA sequence-specific alkylation and the antitumor activity of the alkylating ImPy conjugates using high-resolution denaturing gel electrophoresis and the panel of 39 human cancer cell lines.[29] Recently, we found that alkylating Py–Im polyamides **9** and **10**, which differ only in that the C–H atoms is substituted by an N atom in the second ring, showed significantly different cytotoxicity in the 39 human cancer cell line panel (Fig. 12).[30] The mean log IC_{50} values of **9** and **10** were -6.14 (0.72 μM) and -6.22 (0.60 μM), respectively, which are better than those for mitomycin C (-6.0), and cisplatin (-5.2). A graph of the means showed that the Py–Im conjugates **9** and **10** did not correlate well with each other ($r = 0.65$), confirming the notion that sequence specificity may correlate with their cytotoxicity.

Moreover, the growth inhibitory effects of Py–Im indole-*seco*-CBI conjugates, such as **14** and **17**–**20**, against 10 different cell lines were dramatically different from indole-*seco*-CBI **21** conjugated with various Py–Im polyamides (Fig. 13). These results further confirmed that differences in sequence specificity might affect the pattern of cytotoxicity.[31]

2. Recognizing DNA Structures

Duplex DNA can adopt a variety of sequence-dependent secondary structures, which range from the canonical right-handed B form through to the left-handed Z form.[32] DNA bending and G-quadruplex are also known to exist in vitro.[33] Figure 14 shows the characteristic deviation of DNA structures: the A-form, B-form, Z-form, protein-induced DNA kink, and G-quadruplex. These conformations are assumed to play important biological roles in several processes, such as DNA replication, gene expression and regulation, and repair of DNA damage.[34] Recently, light has again been shed on the biological relevance of Z-DNA. Rich and colleagues have discovered that double-stranded RNA adenosine deaminase (ADAR1),[35] the tumor-associated protein DLM-1,[36] and the E3L[37] protein of vaccinia virus specifically bind to Z-form DNA. Moreover, Liu and colleagues have presented evidence that Z-DNA-forming sequences are required for chromatin-dependent activation of the CSF1 promoter.[38] In addition to the DNA structure itself, the binding of a transcription factor, such as a TATA box binding protein, induces significant DNA bending, which is believed to be essential for the initiation of transcription.[39] For these reasons, investigation of local DNA conformational changes associated with biological events is

indispensable for understanding of the function of DNA.

X-ray crystal analysis and NMR techniques provide structural information about DNA with defined sequences at atomic resolution. Various other spectroscopic methods, such as CD and Raman spectroscopy, can also be used to study DNA structures. These methods deal with model systems of DNA, such as with synthetic oligonucleotides or homopolymers; however, the average conformation of the entire sample is reported, and so, they cannot be used to pinpoint local conformational differences. Moreover, these approaches still cannot be applied directly to probe local DNA structures inside living cells. Although various chemical probes and antibodies have been developed, these methods usually require the isolation of DNA from the nucleus. Because DNA conformational changes are likely to occur in a short period within a living cell, a method that uses the DNA photoreaction and that is capable of fixing DNA conformation in vivo would be very useful. The photoproducts reflecting the DNA local structure should be indicative of the DNA conformational change at sequence resolution during irradiation. In this section, the photoreactivities of 5-halouracil in the five characteristic local DNA structures, that is, the A form, B form, Z form, protein-induced DNA kinks, and G-quadruplexes, are described (Fig. 14). We found that hydrogen abstraction in DNA by the uracil-5-yl generated from the 5-halouracil residue under UV irradiation is atom-specific and highly dependent on the DNA structure. This photochemical method, which reflects DNA structure, could be applied as a unique conformational probe of DNA in living cells.

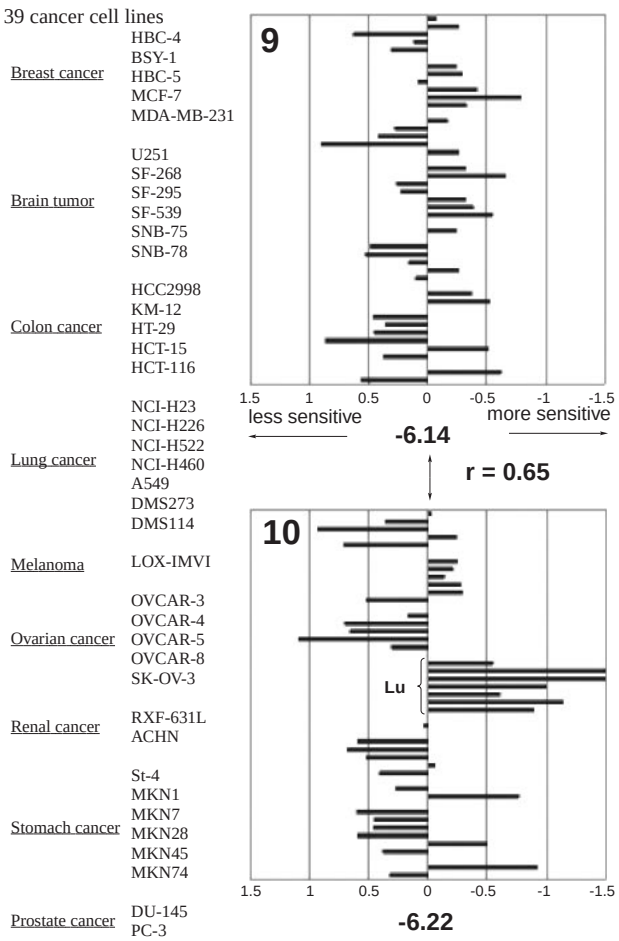

Fig. 12. The IC_{50} profiles by sequence-specific alkylating Py–Im polyamides **9** and **10**, and the correlation coefficient for the mean IC_{50} values.

2.1 Competitive C1′- and C2′α-Hydrogen Abstraction by the Uracil-5-yl Radical B-Form DNA. Replacement of thymine in DNA by 5-halouracil (^{Br}U or ^{I}U) enhances the photosensitivity of the cell with respect to DNA–protein cross-linking, DNA strand breakage, and the creation of alkali-labile sites by forming uracil-5-yl radicals under irradiation conditions.[40] Therefore, we assumed that the photoreactivity of 5-halouracil could be used to probe local DNA conformation. To elucidate the structure of DNA lesions, we started our project by careful product analysis of photoirradiated 5-halouracil-containing hexanucleotides. We found that photoirradiation of the self-complementary B-form duplex $d(GCA^{Br}UGC)_2$ and $d(GCA^{I}UGC)_2$ resulted in the formation of deoxyribonolactone (**1**) as a C2′ oxidation product and erythrose-containing hexamer products **2** as a C2′ oxidation product, together with release of adenine (Fig. 15).[41] Using a C2′ stereospecifically deuterated oligonucleotide of the deoxyribose moiety, we

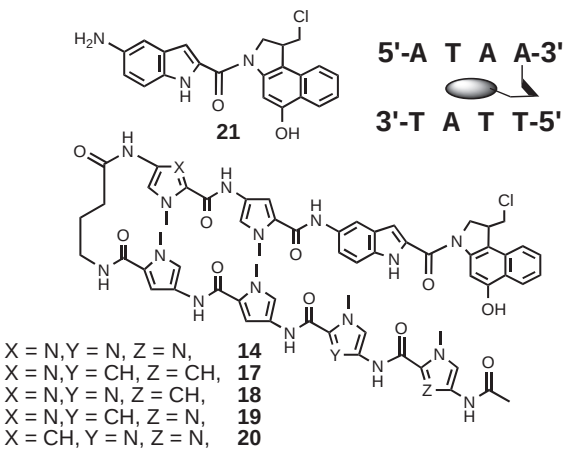

Fig. 13. Chemical structures of the conjugates **14**, **17**–**21**.

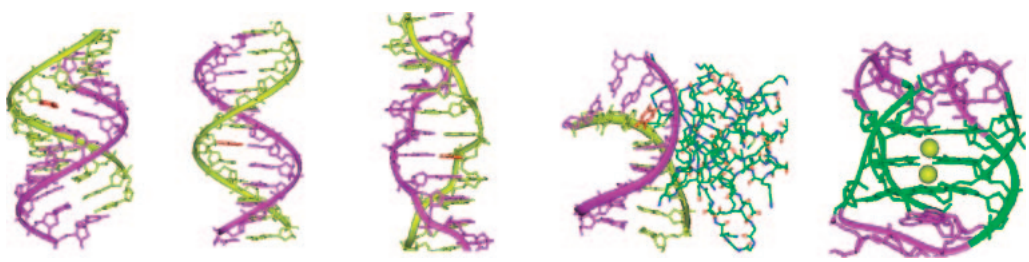

Fig. 14. DNA local structures. From left, B form, A form, Z form, Bent DNA, and G-quadruplex.

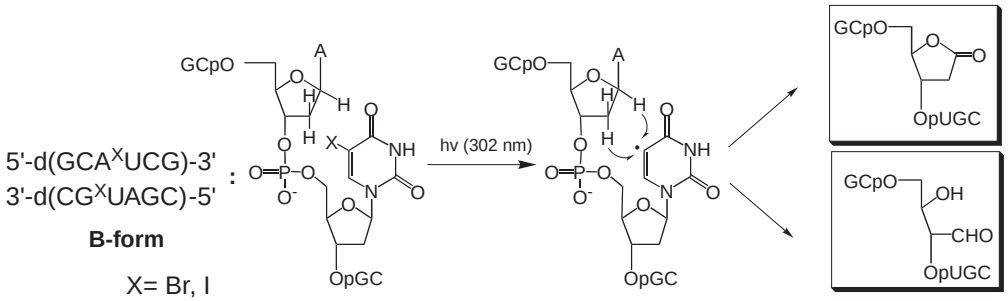

Fig. 15. Competitive C1′ and C2′ hydrogen abstraction in B-form DNA.

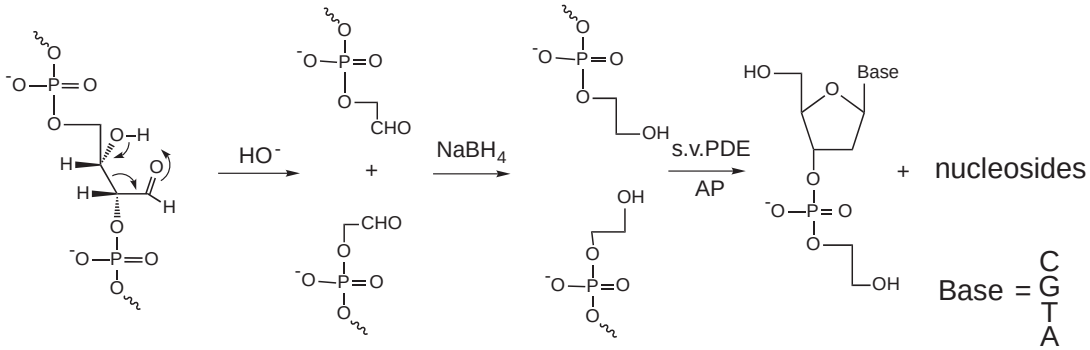

Fig. 16. Detection of C2′ oxidation product in DNA based on retro aldol condensation and subsequent reduction and enzymatic digestion.

demonstrated that the formation of the C2′ oxidation product **2** occurred via a rate-limiting abstraction of the C2′α hydrogen of the deoxyribose moiety by the uracil-5-yl radical. Kinetic isotope effects (k_H/k_D) obtained for the formation of C2′ oxidation product, the erythrose-containing site, by photoirradiation of ^{Br}U- and ^{I}U-containing DNA hexamers were 7.5 and 7.2, respectively.[42] The results clearly indicated that the uracil-5-yl radical competitively abstracted the C1′- and C2′α hydrogens of the deoxyribose residue of A at the 5′ side.

We also demonstrated that erythrose-containing sites in DNA were readily cleaved via retro aldol condensation to give two aldehyde termini under hot alkaline condition. We propose that this method can be used for the detection of C2′ oxidation in DNA (Fig. 16).[41b]

2.2 Selective C1′ Hydrogen Abstraction in A-Form DNA. DNA–RNA hybrid 5′-d(CGA^{I}UGC)-3′/5′-r(GCAUCG)-3′ possessing the A-type structure indicated that the selective C1′ oxidation product **1** was obtained as a major product with release of free adenine (Fig. 17).[43] Similar results were obtained for ^{Br}U-containing DNA–RNA hybrids and for DNA oligomers.[41b] To examine the origin of the selectivity of H abstraction, a putative transition state for H abstraction in a DNA duplex and a DNA–RNA hybrid was constructed, and the conformational energy required to achieve their transition states was evaluated.[43] New sets of parameters of the transition state of H abstraction for the AMBER force field were prepared by ab initio molecular orbital calculations on H abstraction from ethanol by vinyl radicals. In the DNA–RNA hybrid, the minimized energy of the C1′ transition state was the lowest, which explains the observed selective C1′ H abstraction. The calculated structure of the AU step, which contains the putative transition state of C1′ H abstraction in DNA–RNA hybrid, is shown in Fig. 4b. Taking into account the intrinsic susceptibility of H abstraction due to a more stabilized C1′ radical compared with that of C2′ H abstraction, the activation energy level of C1′ and C2′ transition states in the B-form are roughly equivalent, which would explain the observed competitive C1′ and C2′ H abstraction. Although, for a more precise description of H abstraction, the dynamic aspects of the nucleic acids need to be included, the results provide a qualitative explanation of conformation-dependent H abstraction by the uracil-5-yl radical in a DNA duplex and DNA–RNA hybrid.

2.3 Stereospecific C2′α Hydroxylation in Z-Form DNA. Z-form DNA is one of the characteristic and significant local structures of DNA that has been determined by using X-ray crystallography and has been extensively investigated in relation to transcription, the methylation of cytosine, and the level of DNA supercoiling.[44] However, the biological relevance of Z-form DNA is not well understood, presumably because of its short lifetime under torsional stress, which is caused by unwinding of DNA during transcription. Investigating hydrogen abstraction by the uracil-5-yl radical in Z-form DNA, we need to overcome the experimental difficulty in obtaining stable Z-form oligonucleotides under physiological salt conditions. For example, the duplex deoxyoctadecamer d(GmZ^{5}C)$_4$A^{Br}U-(Gm^{5}C)$_4$, which has an A^{Br}U sequence in the middle, retains the typical B-form even in 4 M NaCl solution. To obtain stable Z-form DNA, various modified guanine units were synthesized and introduced into duplex oligonucleotides to evaluate their capacity to stabilize Z-form DNA. It was found that incorporation of 8-methyl-2′-deoxyguanosine (m^{8}G)[45] and 8-methylguanosine (m^{8}rG)[46] into DNA dramatically stabilized the Z-form. The development of the Z-stabilizing monomeric unit, i.e, the Z stabilizer, has allowed us to understand the photoreaction of

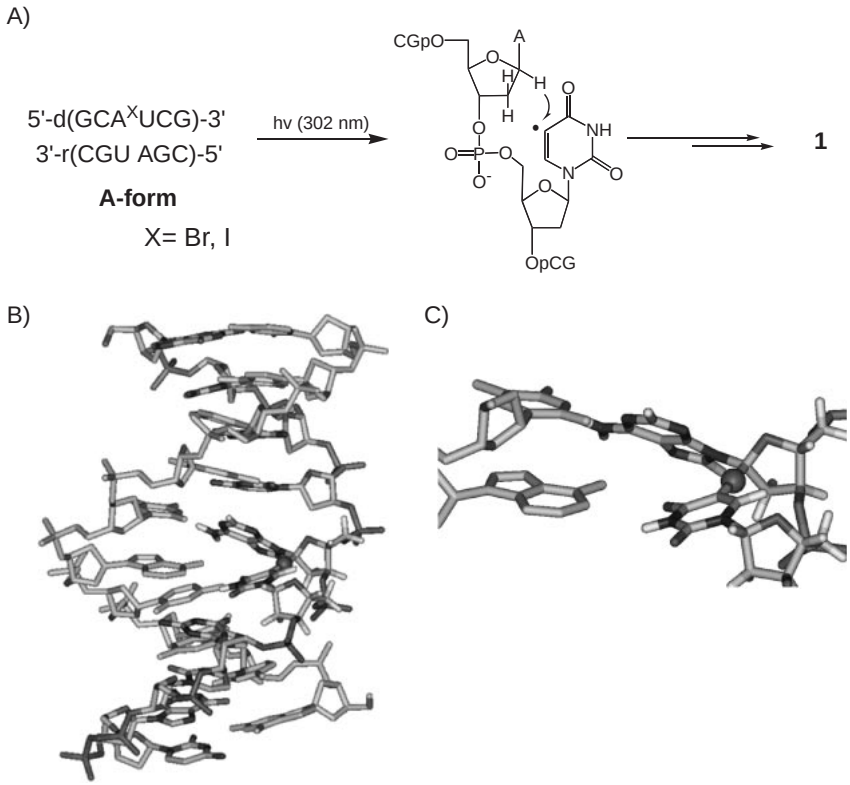

Fig. 17. a) Photoproducts of UV-irradiated hexanucleotides in the A-type DNA–RNA hybrids. Selective 1′-hydrogen abstraction occurred in the A-like structure. b) Structure of A–U step for a minimized octamer which contains the putative transition state of C1′H abstraction in DNA–RNA hybrid and, c) a close-up view of one A–U step.

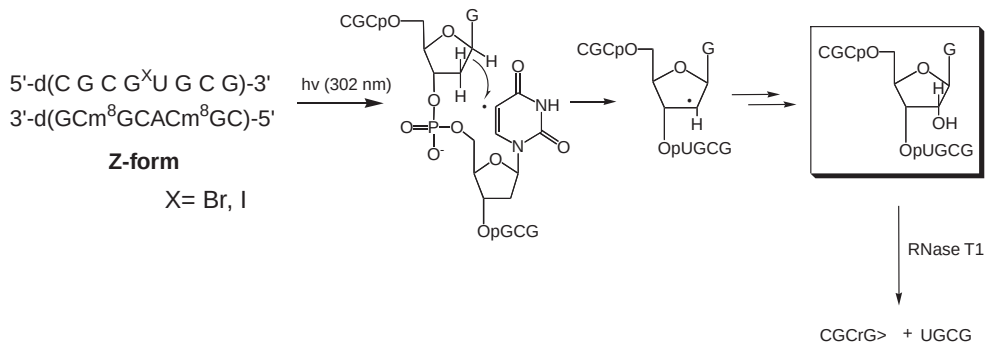

Fig. 18. The reaction of UV-irradiation of d(Cm^{8}GCACm^{8}GCG)/d(CGCG^{I}UGCG) in Z form, indicating that specific 2′β-hydrogen abstraction gives rise to 2′α-hydroxylation. Enzymatic digestion of the hydroxylated product with ribonuclease T_1.

^{I}U in Z-DNA. We found that the ^{I}U-containing Z-form, 5′-d(CGCG^{I}UGCG)-3′/5′-d(Cm^{8}GCACm^{8}GCG)-3′, underwent 2′α-hydroxylation of the duplex under UV irradiation (302 nm), as shown in Fig. 5.[47] Stereospecific 2′β-hydrogen abstraction producing 2′α-hydroxylation (**3**) was demonstrated using a stereospecifically deuterated octanucleotide in Z-form DNA.[48] Importantly, because the 2′α-hydroxylation site in DNA can be easily hydrolyzed by ribonuclease T1, this photochemical and enzymatic hydrolysis is useful for detecting Z-form regions in DNA (Fig. 18).

Recently, Rich and colleagues have discovered that several proteins bind specifically to Z-form DNA, including the ubiquitous enzyme double-stranded RNA adenosine deaminase (ADAR1).[35–37] The possible biological roles of Z-DNA have come to attract much interest. We examined the photoreaction of Z-DNA induced by the binding of Zα, the NH_2-terminus of ADAR1, which is responsible for high-affinity binding to Z-DNA.[35] Stereospecific 2′α-hydroxylation occurred efficiently at the 5′ side of the ^{I}U in the Z form induced by Zα.[49] The X-ray structure of the Zα-d(CGCGCG)$_2$ complex showed that the ribose C2′β-H of the G at the 5′ side is located very close to the uracil-5-yl radical, whereas C1′- and C2′α-H are located very far from the C5 of uracil, as depicted in Fig. 18. The calculated structure of G^{Br}U step, which contains the putative transition state of the C2′β-H abstraction in the Z-DNA, is shown in Fig. 19. These results suggested that, in Z-DNA, Zα packed tightly, with the C3′-endo sugar puckering the G of the duplex, and promoted specific C2′β-H abstraction by

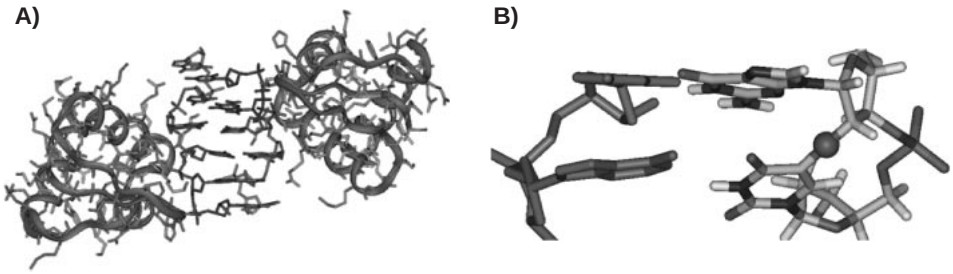

Fig. 19. Structure of the Zα-d(CGCGCG)$_2$ complex based on the X-ray crystal structure (a) and a structure of G-^{Br}U step for a minimized Z-DNA which contains the putative transition state of C2′βH abstraction and a close-up view of one G-^{Br}U step (b).

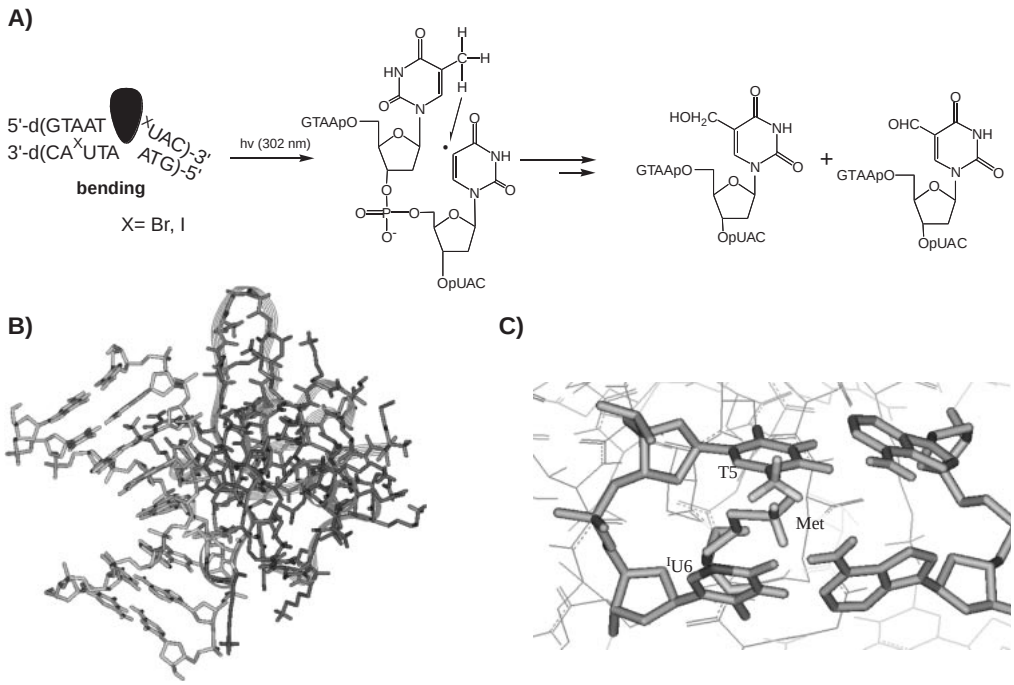

Fig. 20. The reaction of UV-irradiation of d(GTAAT^{I}UAC)$_2$ at DNA kink, indicating that intrastrand hydrogen abstraction gives rise to 5-hydroxymethyluracil and 5-formyluracil-containing octanucleotides (A). Structure of the d(GTAAT^{I}UAC)$_2$–Sso7d complex based on the X-ray crystal structure (B) and a close-up view of the reacting region (C).

the uracil-5-yl radical to omit C1′ and C2′ oxidation.

2.4 Hydrogen Abstraction from the 5-Methyl Group of Thymine at DNA Kinks. The binding of a protein often induces significant DNA conformational changes, which are thought to play important biological roles.[32,33] For example, the TATA box binding protein induces DNA bending that is essential for the initiation of transcription. To detect the DNA kink induced by protein binding, the photoreaction of 5-halouracil-containing DNA in the presence of Sso7d protein was examined. Sso7d is a small chromosomal protein from the hyperthermophilic archaeabacterium *Sulfolobus solfataricus*, which exhibits high thermal, acid and chemical stability. The crystal structure of the complex of Sso7d and d(GTAATTAC)$_2$ has been solved at high resolution.[50] The protein binds in the minor groove, causing a sharp bending (60°) at the TpT step; this kink results from the intercalation of the hydrophobic side chains of Val26 and Met29. Consistent with previous observations involving B-form DNA, photoirradiation of d(GTAAT^{I}UAC)$_2$ produced C1′ and C2′ oxidation products in the absence of Sso7d. In the presence of Sso7d, the formation of 5-hydroxymethyluracil- and 5-formyluracil-containing octanucleotides was observed (Fig. 20).[51] These results clearly indicated that the protein-induced DNA kink caused intrastrand hydrogen abstraction from the 5-methyl group of thymine. Inspection of the X-ray structure indicated that the T5-Me was in close proximity to the uracil-5-yl radical, whereas the T5-C1′H and T5-C2′H are located far from the adjacent uracil-5-yl radical, as shown in Fig. 20C. We concluded that the unusual intrastrand H abstraction from T5-Me by the radical occurred efficiently at the observed bending site in the crystal structure.[50] This specific-intrastrand methyl H abstraction provides a powerful tool to detect directly DNA kinks in solution.

HPLC analysis of the photoirradiated d(GTAAT^{I}UAC)$_2$–Sso7d complex also indicated that the Sso7d was efficiently oxidized to Sso7dOH. Lysyl endopeptidase-treated Sso7dOH showed that the oxidation occurred mainly at the fragment from residues 29 to 40 (78%). Post source decay (PSD)–MS/MS indicated that specific photo-oxidation occurred at Met29 during photoirradiation of the d(GTAAT^{I}UAC)$_2$–Sso7d complex. Inspection of the X-ray structure suggested that res-

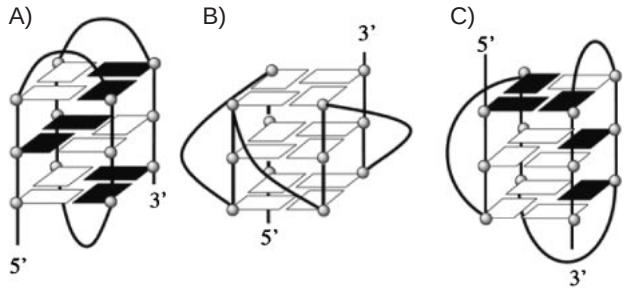

Fig. 21. Schematic representations of the folded structures of d[$AG_3(T_2AG_3)_3$]. (a) The Na^+-stabilized solution structure, with one diagonal and two lateral TTA. (b) The K^+-stabilized crystal structure, with TTA external loops abutting the sides of the G-quartet and parallel GGG columns. (c) The mixed chair structure determined by 8-Br-guanine substitution and CD spectroscopy. Guanine residues in syn conformation are shown in black.

idue Met29 was in close proximity to the uracil-5-yl radical, which was intercalated with the major groove at the bending site in the crystal structure. These results suggested that the interaction of DNA–Sso7d in solution is substantially similar to its crystal structure.

2.5 Efficient C1′ Hydrogen Abstraction in the Antiparallel G-Quadruplex. G-quadruplexes are four-stranded DNA structures formed by G-rich sequences.[52] Although G-quadruplexes have so far been studied only in vitro, they are attracting increasing attention because of their postulated involvement in a variety of biological processes. The DNA of human telomeres consists of repeats of the nucleotide sequence TTAGGG, ending in a single-stranded segment that overhangs at the end of the double-stranded DNA helix. The single-stranded repeats can form four-stranded G-quadruplex structures.[53] NMR analysis has demonstrated that the solution structure of a 22-mer of 5′-d[$AGGG(TTAGGG)_3$]-3′ in the presence of Na^+ ions possesses an antiparallel G-quadruplex structure, in which the opposing GGG columns are antiparallel with one diagonal and two lateral TTA loops (Fig. 21).[54] In contrast, the same 22-mer adopts a completely different G-quadruplex architecture in a crystal grown in the presence of K^+ ions, in which four core GGGs are parallel, with the three linking external loops positioned on the exterior of the G-quartet core.[55] Using 8-Br-guanine-substitution, we recently determined the topology of the 22 mer as a mixed chair form by CD spectroscopy.[56]

To explore the structure-dependent hydrogen abstraction in antiparallel and parallel G-quadruplex, one of the six thymine (T) residues in 22-mer human telomeric DNA 5′-d(AGGG-T_1T_2AGGGT_3T_4AGGGT_5T_6AGGG)-3′ was substituted with ^{I}U to generate six types of oligodeoxynucleotide (ODNs 1–6).[57] Under UV irradiation, more than 60% of antiparallel ODN 4, in which T_4 in the middle of the diagonal loop was substituted with ^{I}U, was consumed. In marked contrast to the photoreactivity of the antiparallel ODN 4, the parallel ODNs 1–6 were not consumed (<2%) under the same irradiation conditions. Product analysis indicated that 2′-deoxyribonolactone was efficiently produced with release of thymine from photoirradiated ODN 4 in the antiparallel structure (Fig. 22).

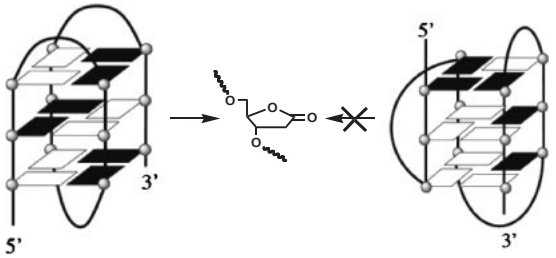

Fig. 22. Formation of ribonolactone containing 22 mer from photoirradiated oligonucleotide d(AGGGTTAGGG-T^IUAGGGTTAGGG) (ODN 4) in Na^+-form not from K^+-form.

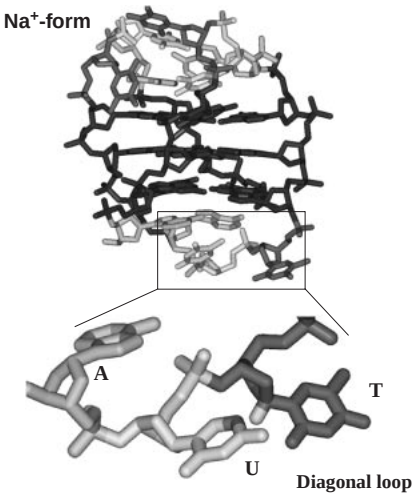

Fig. 23. Structure of photoirradiated d(AGGGTTAGGG-T^IUAGGGTTAGGG) (ODN 4) based on the NMR structure (Na^+-form), and a close-up view of the loop region.

The high photoreactivity of ODN 4 in the antiparallel G-quadruplex can be explained by comparing the loop regions of the antiparallel structure (Fig. 23).[54] In the antiparallel G-quadruplex, uracil-5-yl radical and C1′ H are in close proximity in the diagonal loop structure of the antiparallel G-quadruplex, thereby allowing C1′-hydrogen abstraction by the uracil-5-yl radical in the loop. Furthermore, the NMR structure suggests that the uracil-5-yl radical is positioned closer to the C1′ hydrogen of the adjacent T_3 than the other hydrogens in the lateral loop.

Our data indicated that the hydrogen abstraction of DNA by the uracil-5-yl radical generated from 5-halouracil under irradiation was atom specific and highly dependent on DNA conformation (Fig. 24). Competitive C1′- and C2′α-hydrogen abstractions were observed in B-DNA, whereas selective 1′-hydrogen abstraction occurred in the A-like structure of DNA–RNA hybrids. In Z-form DNA, stereospecific C2′β-hydrogen abstraction gave rise to C2′α-hydroxylation. In protein-induced DNA kinks, photoirradiation caused intrastrand hydrogen abstraction from the 5-methyl group of thymine at the 5′ side. The photoreactivity of ^{I}U-containing telomeric DNA depended on the orientation of the G-quartet: the 2′-deoxyribonolactone residue was effectively produced only in the diagonal loop of the antiparallel G-quartet. These studies determined the detailed relationship between the DNA local structure and pho-

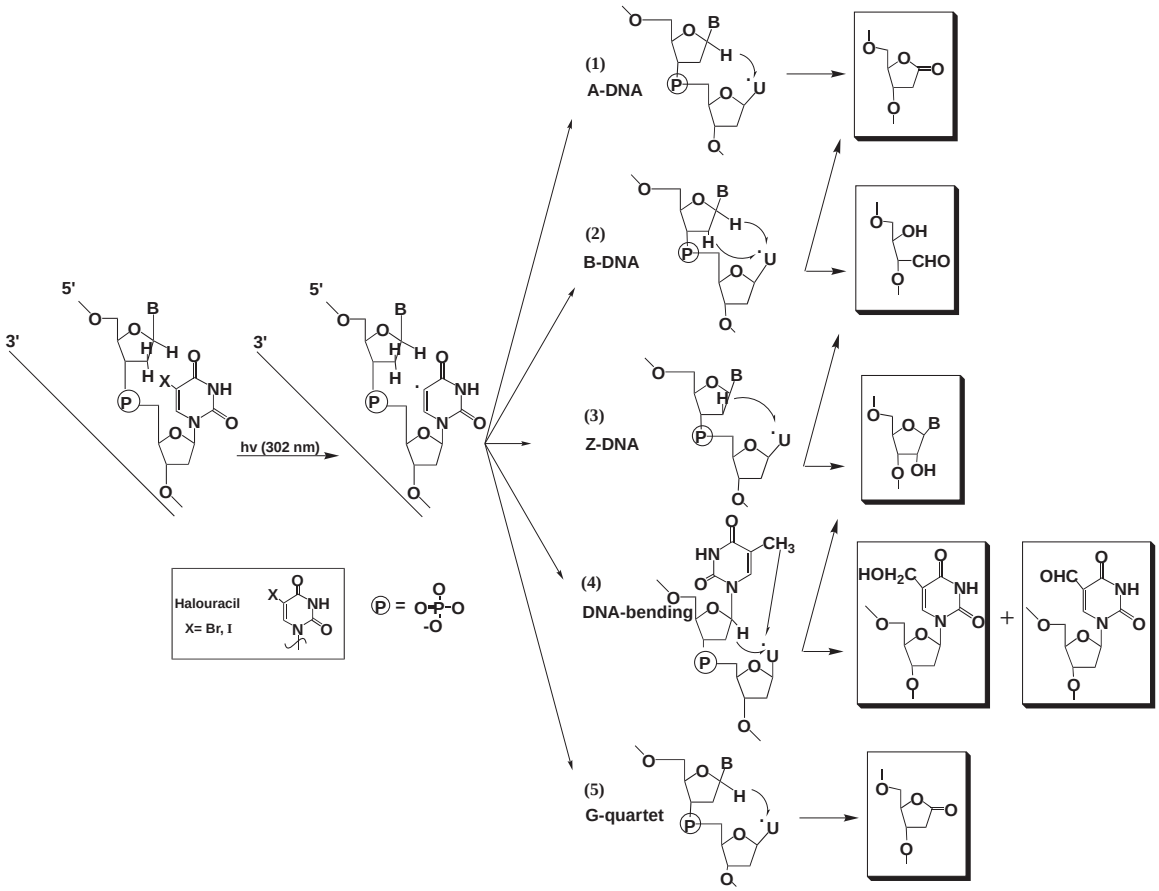

Fig. 24. Uracil-5-yl radical generated from 5-halouracil under UV irradiation carried out structure dependent atom specific hydrogen abstraction on various important DNA local structures.

toproduct and showed the potential of this photochemical method in detecting DNA structure. Ligation-mediated polymerase chain reaction (LMPCR) is a useful technique to detect photoproducts in vivo.[58] Because 5-halouracil-substituted DNA is functional in living-cell systems, such as *E. coli*, use of the photochemical reactions of 5-halouracil-containing DNA would provide a powerful tool to probe local DNA conformations in vivo.

3. Electronic Structure of DNA

Recently, there has been growing interest in the use of DNA as a nanomaterial, as DNA fragments with defined sequence can be prepared chemically and enzymatically. Charge transfer along DNA is currently of intense interest because it is related to DNA damage and repair, and the use of DNA as a nanodevice. DNA has four bases—C, G, T, and A—with different electronic properties. Extensive research has demonstrated that charge transfer along DNA dramatically depends on base sequence as well as the stacking orientation of DNA structures.

3.1 Oxidation of Guanine in B-DNA. The genome is constantly assaulted by endogenous and exogenous oxidative stress. Independent of the source, reactive species are potent genotoxins that attack duplex DNA and generate oxidative lesion products. These genotoxin-induced alterations in the genomic message have been implicated in aging and cancer. From bacteria to humans, various types of repair enzymes maintain the integrity of the genome. Therefore, considerable

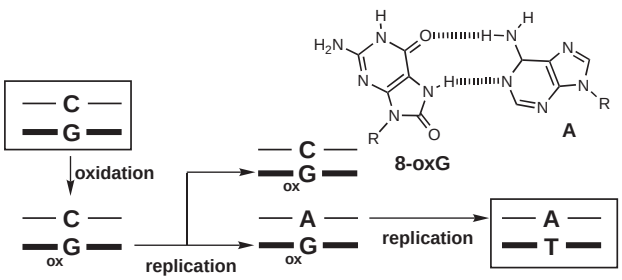

Fig. 25. Proposed mechanism of GC → TA transversion mutation caused by 8-oxoG.

effort has focused upon understanding the mechanisms of oxidative DNA damage and repair.[59] Currently, over 50 oxidative DNA lesions have been characterized.[60] Guanine is highly susceptible to one-electron oxidation by singlet oxygen and peroxynitrite,[61] because it has the lowest redox potential among four bases.[62] A typical lesion product is 8-oxoguanine (8-oxoG), which is formed under various oxidative conditions (Fig. 25). Thus, the biological impact of 8-oxoG has been extensively investigated.[63] It is well documented that 8-oxoG causes G–C to T–A transversions by forming specific base pair with adenine (Fig. 25).[63e]

In contrast to the G–C to T–A transversions, molecular mechanism for G–C to C–G transversions has not been well understood, even though they frequently occurs. Previously,

our laboratories have demonstrated that naphthalimide derivative selectively generates piperidine-sensitive alkaline labile sites at the 5′-guanine (G) of 5′-GG-3′ sequence with a lower frequency at the 5′-G of 5′-GA-3′ sequence upon 366 nm photoirradiation.[64] A similar 5′-GG-3′ specificity for the formation of alkaline labile sites has been observed for the photoirradiation in the presence of various types of photocleaving molecules, including $Co(NH_3)_6^{3+}$, riboflavin, benzophenone, and anthraquinone derivatives as well as for the direct irradiation of DNA with 193 nm excimer laser. The common pattern of these 5′-GG-3′ specific DNA cleavage strongly suggests that such specificity is not determined by the binding orientation of the photocleaving molecules but must be originated from a common intrinsic chemical property of DNA itself, which has not been well recognized. Ab initio molecular orbital calculations of stacked DNA bases with various orientations indicate that stacking of two guanine bases significantly lowers the ionization potential and that the HOMO of the stacked 5′-GG-3′ is localized mainly on the 5′-G in B form DNA (Fig. 26).[65]

3.2 The Generation and Mutagenicity of Imidazolone. Iz and Oz are major products of guanine via one-electron photo-oxidation using photosensitizers, such as benzophenone, riboflavin, and anthraquinone.[66] We have recently demonstrated that Iz is a key UV-detectable product formed in double-stranded DNA during photo-oxidation with riboflavin. Photosensitization of 8-oxoG with riboflavin also provides Iz and Oz preferentially under basic conditions (Fig. 27).[67] Molecular orbital calculations suggested that π-stacking in B form DNA significantly enhanced the reactivity of 8-oxodG[68] in a similar manner as G at GG step.[65] In fact, Cadet et al. have demonstrated that guanine is not oxidized until 8-oxoG is completely oxidized using monomer.[69] Thus, the amount of 8-oxoG does not directly reflect the strength of oxidative stress, even though it is a useful marker for it. Since 8-methoxyguanine has a low oxidation potential similar to 8-oxoG, it is a useful synthetic precursor for Iz.[70] Iz-containing sites can be generated at specific sequences using UV irradiation in the presence of riboflavin.

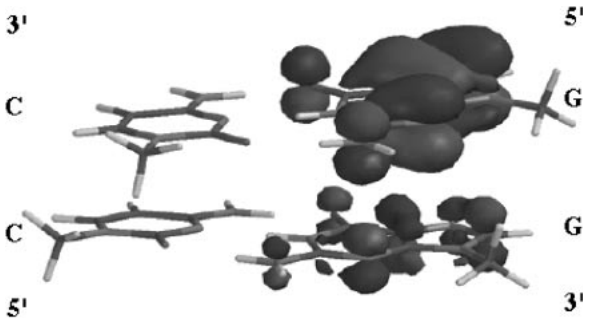

Fig. 26. 5′-Localization of HOMO of stacked GG bases in B-DNA.

Long-range guanine oxidation at GG and GGG sequences, through a DNA base π-stack, has been observed using a range of tethered oxidants,[71] such as anthraquinone and phenanthroline Ru or Rh complexes, and 8-oxoG is an oxidation product of this system.[72] Here, the contributions of singlet oxygen and hydroxyl radical are negligible. We photo-irradiated a covalently anthraquinone-linked oligomer with a complementary oligomer containing 8-oxoG and found that Iz was produced from 8-oxoG through long-range hole migration.[73] Importantly, the H-bonding donor and acceptor abilities of Iz closely resemble cytosine; Iz is assumed to be able to form base pairs with guanine (Fig. 28). The estimated stabilization energy of an Iz–G base pair by ab initio molecular orbital calculations in vacuo and in water showed that the stabilization energy of Iz–G is similar to that of C–G.[66b,73]

Though primer extension by DNA polymerase, we showed that only guanine was specifically incorporated opposite Iz.[73] However, in contrast, non-mutagenic cytosine was incorporated opposite 8-oxoG, in addition to mutagenic incorporation of adenine. Kinetic analysis indicated that the frequency of guanine incorporation opposite Iz was similar to that of adenine incorporation opposite 8-oxoG. Although the efficiency of chain extension from the Iz–G pair was lower than that from 8-oxoG–A base pairs in the kinetic analysis, the yield of translesions across Iz was similar to that across 8-oxoG. Thus, the Iz–G base pairing possibly occurs during replication, and Iz may explain G–C to C–G transversions (Fig. 29). In addition, the "reverse" approach consisting of DNA polymerization

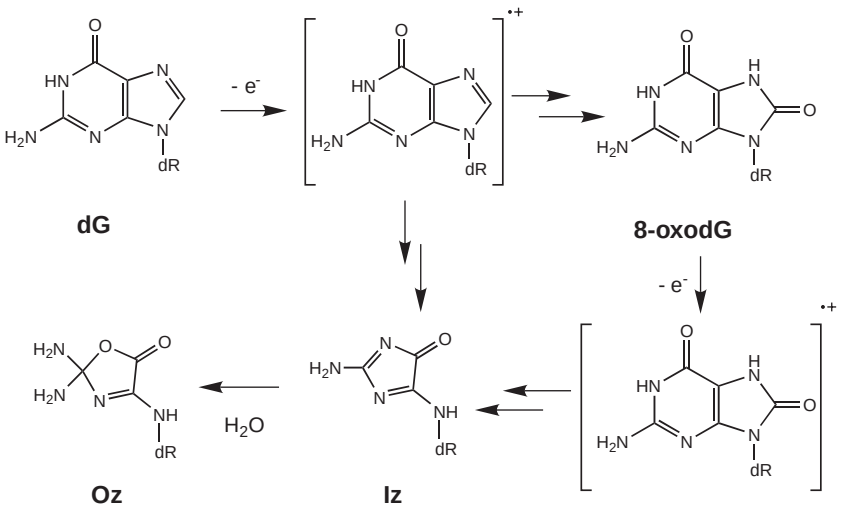

Fig. 27. Proposed scheme for the formation of 8-oxoG, Iz and Oz from one electron oxidation of dG.

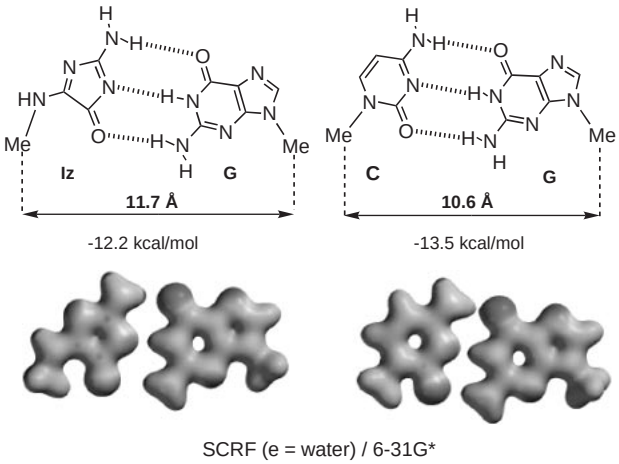

Fig. 28. The proposed Iz–G and Watson–Crick C–G base pairs and electrostatic populations Iz–G and C–G base pairs. The base pairs were calculated using Gaussian 94 and Spartan (version 5.0) programs. The geometry was optimized at the 6-31G* level.

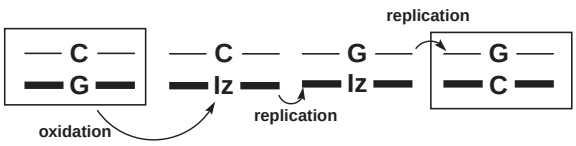

Fig. 29. Proposed mechanism of GC → CG transversion mutation caused by Im.

using dIzTP showed that Iz was incorporated opposite guanine. The results confirmed the possible formation of Iz–G base pairs.

3.3 Examination of Electron-Transfer Process Using ^{Br}U. The photoreactivity of 5-halouracil-containing DNA was investigated using uniformly ^{X}U-substituted DNA fragments under 302 nm irradiation. In contrast to the fact that photoirradiation of d(GCA^{Br}UGC)$_2$ gives rise to efficient formation of C1′ and C2′ oxidation products, hexanucleotides that do not have an A^{Br}U sequence, such as 5′-d(GCG^{Br}UCG)-3′/5′-d(CGACGC)-3′, showed very poor photoreactivity. Based on these results, we initially proposed a mechanism, in which sequence-specific electron transfer occurs from the adjacent A at the 5′ side to ^{Br}U, forming the ^{Br}U anion radical in the duplex structure. Forming a uracil anion radical eliminates the Br anion to generate a uracil-5-yl radical that abstracts the C1′ hydrogen of A, and subsequent oxidation of the C1′ radical by the cation radical of A produces ribonolactone via a C1′ cation. The Greenberg group has also confirmed this type of selectivity.[74] Since G is a better electron-donating base, the reactivity has been labeled a "contrathermodynamic reaction." Recently, ^{Br}U was used as a probe of excess electron transfer.[75] We investigated the electron transfer along DNA using uniformly 5-halouracil substituted DNA.[76] Using PCR, we prepared DNA fragments, in which all thymine residues were substituted with ^{Br}U or ^{I}U. The DNA fragments were irradiated with monochromatic 302 nm UV light and then analyzed on sequencing gels. Surprisingly, specific cleavage at 5′-(G/C)AA^{X}U^{X}U-3′ and 5′-(G/C)A^{X}U^{X}U-3′ sequences in both ^{Br}U- and ^{I}U-containing DNA fragments was observed only after heat treatment. HPLC product analysis of oligonucleotides indicated that the major products were ribonolactone-containing octamer. When oligonucleotides were irradiated in $H_2{}^{18}O$, incorporation of ^{18}O atoms into ribonolactone residues from the $H_2{}^{18}O$ was observed, indicating that H_2O is the source of the carbonyl oxygen of the ribonolactone. From these observations, we have proposed a possible mechanism for the efficient photoreactions at 5′-GAA^{X}U^{X}U-3′ sequences (Fig. 30). Initial electron transfer would occur from G to the electron-deficient ^{X}U^{X}U step through stacked AA and A.[76] Release of the halide anion from the ^{X}U^{X}U anion radical generates uracil-5-yl radicals, which abstracts the C1′ hydrogen from the adjacent A of the ^{X}U^{X}U step. One electron oxidation of the C1′ radical of dA by the cation radical of G gives rise to a C1′ cation and regeneration of guanine. The intervening A bases between G and the ^{X}U^{X}U step are considered to act as a bridge between the electron donor and acceptor for charge separation after electron transfer from G to the ^{X}U^{X}U step, thus preventing rapid back electron transfer. Previously observed A^{Br}U sequence specificity can be explained by the same role of adenine.

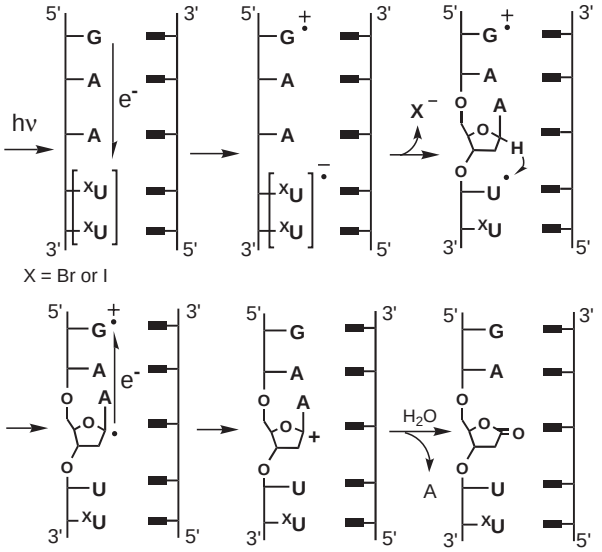

Fig. 30. Proposed mechanism for the efficient photoreaction at 5′-(G/C)AA^{X}U^{X}U-3′ sequence.

3.4 Four Base π-Stack in Z-DNA. In contrast, the photoreactivity of 5′-CGCG^{Br}UGCG-3′/5′-CmGCACmGCG-3′ in Z-DNA is completely different from B-DNA. Z-form DNA underwent efficient photoreaction to provide rG-containing DNA.[77] The results clearly indicate that structural changes caused by the B–Z transition dramatically increased the photoreactivity of ^{Br}U-containing DNA. Inspection of the molecular structure of the Z-form suggested that unique four-base π-stacks were formed at the G$_4$-^{Br}U$_5$-C$_{11}$-G$_{10}$ sequence, whereas there is a continuous π-stack along each strand in B-DNA. Interestingly, G in the complementary strand was oxidized to the Im-containing DNA. These results suggested the intriguing possibility that the G$_{10}$ in a complementary strand located at the end of the four-base π-stacks act as an electron donor. In addition, they clearly indicated that the interstrand charge-transfer from mG$_{10}$ to ^{Br}U$_5$ initiated the photoreaction. A proposed mechanism for the photoreaction of ^{Br}U-containing Z

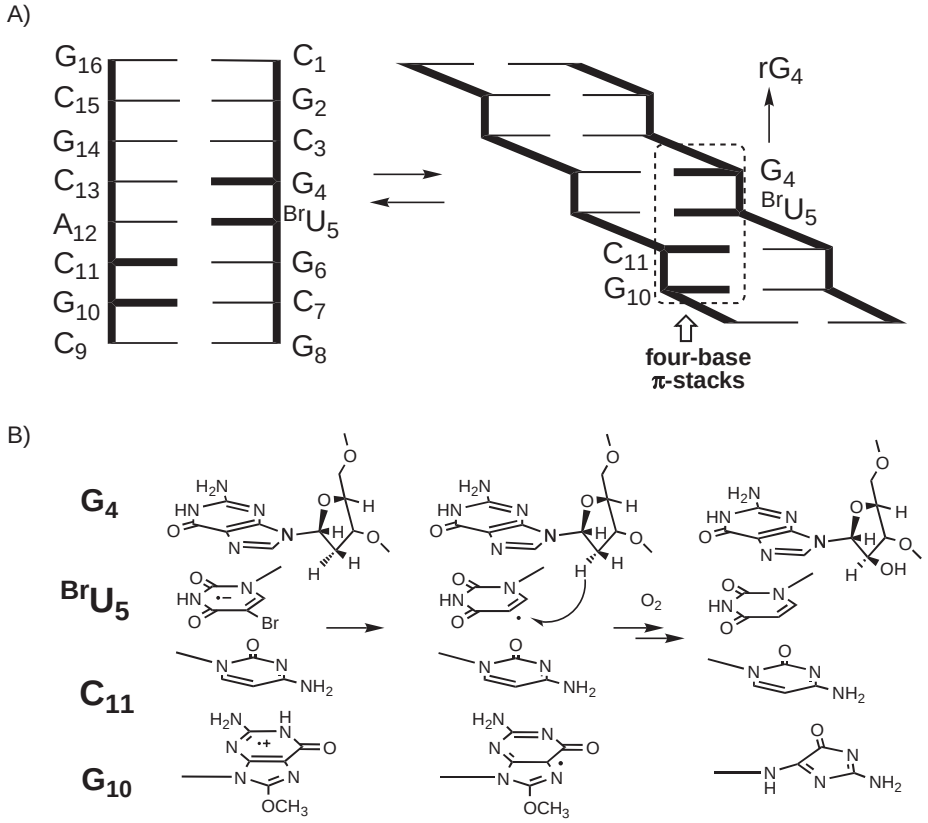

Fig. 31. Different π-stacking in B- and Z-DNA. (A) Schematic presentation of continuous π-stacking in B-DNA and four-base π-stacks in Z DNA in which an efficient electron transfer from G_{10} to $^{Br}U_5$ occurs. (B) Proposed mechanism for the photoreaction ^{Br}U-containing Z DNA.

DNA is shown in Fig. 31. Under irradiation conditions, efficient electron transfer from G_{10} to $^{Br}U_5$ in four-base π-stacks produces cationic and anionic radicals. The anionic radical of ^{Br}U eliminates bromine to generate a uracil-5-yl radical, which abstracts hydrogen to produce the rG residue. Cationic radicals of G or methoxyG generate Im.

3.5 Monitoring Conformational Change of B–Z Form Using Aminopurine. We expected that different π-stacks influenced the electronic properties between B- and Z-DNA. We used aminopurine (Ap) as a probe for charge-transfer within DNA duplexes, where the purine (G and A) and pyrimidine (C and T) bases function as donors and acceptors, respectively. Thus, the fluorescence intensity of the Ap-containing duplex decamer was monitored under various conditions. In 1 M NaCl, this oligomer existed in the B-conformation and showed very weak fluorescence. However, the fluorescence of this decamer increased proportionally when the ratio of Z-conformation was increased by increasing the NaCl concentration.[78] These results indicated that the restricted charge-transfer between different four-base π-stacks of Z-DNA compared with B-DNA could be monitored by the fluorescence of Ap. We also designed a molecular thermometer based on the change in electronic properties when converting from B- to Z-DNA. It is known that the equilibrium between the Z- and the B-conformations can be controlled using temperature (Fig. 32). At low temperature, the proportion of the Z-conformation is high, due to its lower entropy. Thus, the fluorescence of the oligomer was monitored at different temperatures. The intensity of the fluorescence correlated with the temperature. At 32 °C, where 23% of the oligomer was in the Z-conformation, the fluorescence of the oligomer was very weak, whereas the fluorescence dramatically increased at 2 °C, where 53% of the oligomer was in the Z-conformation. Under repetitive temperature changes, a reproducible fluorescence change was observed, meaning that the B–Z transition induced by a change in

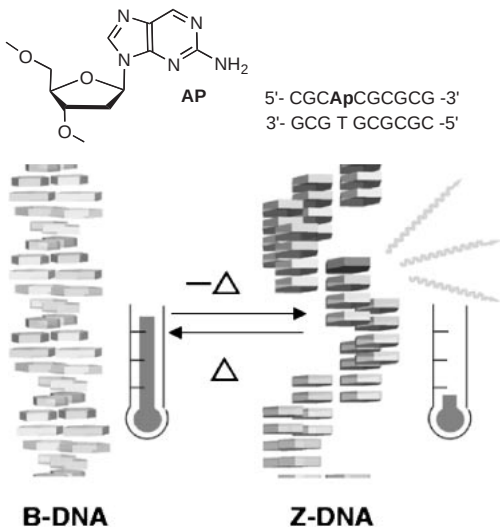

Fig. 32. The concept of nanothermometer based on the difference between B- and Z-DNA.

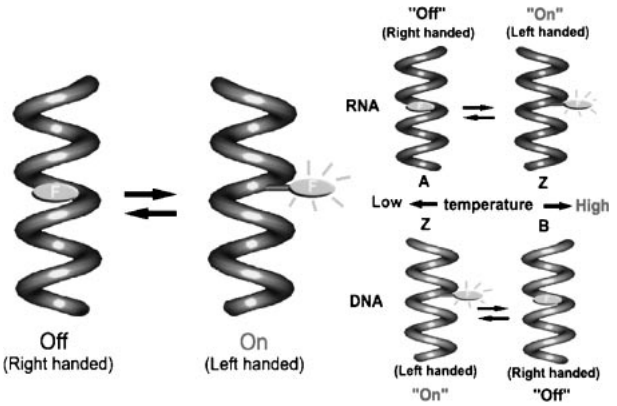

Fig. 33. Schematic representation of RNA and DNA reversible molecular devices that respond inversely to thermal stimulation.

temperature can be readily monitored by the fluorescence intensity of Ap. To the best of our knowledge, this is the first demonstration of the control of charge-transfer caused by the alteration of π-stacks in DNA induced by conformational change.

3.6 Biomolecule-Based Switching Devices that Respond Inversely to Thermal Stimuli. Surprisingly, these phenomena were completely inverted in RNA.[79] At higher temperatures, RNA converted to the Z form to enhance emission. At low temperature, DNA emitted fluorescence and at high temperature, RNA emitted fluorescence. The response of this RNA and DNA device to thermal stimuli was completely reversible. Because both RNA and DNA show stronger fluorescence in the Z form than in the A and B form, these DNA and RNA devices together can serve as a "right–left" or "off–on" switch. By using the different properties of DNA and RNA, we successfully constructed molecular devices that showed completely inverted responses to temperature (Fig. 33), which were the first examples of reversible switching devices with inverted responses to be the same stimulus. This switching may provide a new programming and sensing system for nano-devices.

Conclusion

We have been examined DNA with respect to the sequence read out and its intrinsic reactivity based on electronic property of DNA. Based on the investigation of DNA modification by natural products, we have successfully developed Py–Im hairpin polyamide conjugates that precisely alkylate DNA at specific matching sequences at nanomolar concentrations. The selectivity and the efficiency of DNA alkylation were higher than those of DNA-alkylating antibiotics. Preliminary examination of cytotoxicity using a nude mouse xenograft model revealed that alkylating Py–Im conjugate inhibits the growth of a human breast cancer cell lines, suggesting that Py–Im polyamides targeting specific sequences in individual cancer cell lines will provide a promising methodology for the development of tailor-made antitumor drugs. Our data of photoreaction of 5-halouracil-containing DNA indicated that hydrogen abstraction from DNA by the uracil-5-yl radical generated from 5-halouracil under irradiation was atom specific and highly dependent on DNA conformation. These studies determined the detailed relationship between the DNA local structure and photoproduct and showed the potential of this photochemical method in detecting DNA structure. Ligation-mediated polymerase chain reaction (LMPCR) is a useful technique to detect these products in vivo.[80] Because 5-halouracil-substituted DNA is functional in living-cell systems, use of the photochemical reactions of 5-halouracil-containing DNA would provide a powerful tool to probe local DNA conformations in vivo. During our investigation, I realized that although these reactions in macromolecules are completely different from those in monomeric components and proceeds in aqueous solution, most of the reactions there can be understand as combinations of typical organic chemistry textbook reactions. Knowledge of reactivity of DNA is very important to understand mutation, carcinogenesis and design of antitumor agnets.

I would like to express my sincere appreciation to all the coworkers, whose names are cited in the references, without whose dedication, hard work and enthusiasm for science, this accounts would not have been possible. Accounts are dedicated to Professor Isao Saito on the occasion of his 65th birthday. This work was supported by a Grant-in-Aid for Priority Research from the Ministry of Education, Culture, Sports, Science and Technology, Japan; and SORST of Japan Science and Technology (JST).

References

1 a) I. Saito, H. Sugiyama, S. Ito, N. Furukawa, T. Matsuura, *J. Am. Chem. Soc.* **1981**, *103*, 1598. b) I. Saito, H. Sugiyama, T. Matsuura, *J. Am. Chem. Soc.* **1983**, *105*, 956. c) I. Saito, H. Sugiyama, T. Matsuura, *J. Am. Chem. Soc.* **1983**, *105*, 6989. d) I. Saito, H. Sugiyama, T. Matsuura, K. Ueda, T. Komano, *Nucleic Acids Res.* **1984**, *12*, 2879. e) I. Saito, T. Matsuura, *Acc. Chem. Res.* **1977**, *10*, 346.

2 a) H. Sugiyama, R. E. Kilkuskie, S. M. Hecht, G. A. van der Marel, J. H. van Boom, *J. Am. Chem. Soc.* **1985**, *107*, 7765. b) H. Sugiyama, R. E. Kilkuskie, L.-H. Chang, L.-T. Ma, S. M. Hecht, G. A. van der Marel, J. H. van Boom, *J. Am. Chem. Soc.* **1986**, *108*, 3852. c) G. M. Ehrenfeld, J. B. Shiply, D. C. Heimbrook, H. Sugiyama, E. C. Long, J. H. van Boom, G. A. van der Marel, N. J. Oppenheimer, S. M. Hecht, *Biochemistry* **1987**, *26*, 931.

3 a) H. Sugiyama, C. Xu, N. Murugesan, S. M. Hecht, *J. Am. Chem. Soc.* **1985**, *107*, 4104. b) H. Sugiyama, C. Xu, N. Murugesan, S. M. Hecht, G. A. van der Marel, J. H. van Boom, *Biochemistry* **1988**, *27*, 58.

4 a) I. Saito, T. Morii, H. Sugiyama, T. Matsuura, C. F. Meares, S. M. Hecht, *J. Am. Chem. Soc.* **1989**, *111*, 2307. b) H. Sugiyama, H. Kawabata, T. Fujiwara, Y. Dannoue, I. Saito, *J. Am. Chem. Soc.* **1990**, *112*, 5252. c) H. Sugiyama, K. Ohmori, I. Saito, *J. Am. Chem. Soc.* **1994**, *116*, 10326.

5 a) H. Kawabata, H. Takeshita, T. Fujiwara, H. Sugiyama, T. Matsuura, I. Saito, *Tetrahedron Lett.* **1989**, *30*, 4263. b) I. Saito, H. Kawabata, T. Fujiwara, H. Sugiyama, T. Matsuura, *J. Am. Chem. Soc.* **1989**, *111*, 8302. c) H. Sugiyama, T. Fujiwara, H. Kawabata, I. Saito, N. Hirayama, N. Yoda, *J. Am. Chem. Soc.* **1992**, *114*, 5573.

6 K. L. Chan, H. Sugiyama, I. Saito, *Tetrahedron Lett.* **1991**, *32*, 7719.

7 a) H. Sugiyama, M. Hosoda, I. Saito, A. Asai, H. Saito,

Tetrahedron Lett. **1990**, *31*, 7197. b) H. Sugiyama, K. Ohmori, K. L. Chan, M. Hosoda, A. Asai, H. Saito, I. Saito, *Tetrahedron Lett.* **1993**, *34*, 2179.

8 T. Fujiwara, I. Saito, H. Sugiyama, *Tetrahedron Lett.* **1999**, *40*, 315.

9 X. Gao, A. Stassinopoulos, J. S. Rice, I. H. Goldberg, *Biochemistry* **1995**, *34*, 40.

10 a) K. Yamamoto, H. Sugiyama, S. Kawanishi, *Biochemistry* **1993**, *32*, 1059. b) H. Sugiyama, C. Lian, M. Isomura, I. Saito, A. H.-J. Wang, *Proc. Natl. Acad. Sci. U.S.A.* **1996**, *93*, 14405.

11 T. Fujiwara, Z.-F. Tao, Y. Ozeki, I. Saito, A. H.-J. Wang, M. Lee, H. Sugiyama, *J. Am. Chem. Soc.* **1999**, *121*, 7706.

12 R. P. L. de Clairac, B. H. Geierstanger, M. Mrksich, P. B. Dervan, D. E. Wemmer, *J. Am. Chem. Soc.* **1997**, *119*, 7909.

13 Z.-F. Tao, T. Fujiwara, I. Saito, H. Sugiyama, *J. Am. Chem. Soc.* **1999**, *121*, 4961.

14 a) A. Y. Chang, P. B. Dervan, *J. Am. Chem. Soc.* **2000**, *122*, 4856. b) N. R. Wurtz, P. B. Dervan, *Chem. Biol.* **2000**, *7*, 153. c) B. Purnell, A. Sato, A. O'kelley, C. Price, K. Summerville, S. Hudson, C. O'hare, K. Kiakos, T. Asao, M. Lee, J. A. Hartley, *Bioorg. Med. Chem. Lett.* **2006**, *16*, 5677. d) A. Sato, L. McNulty, K. Cox, S. Kim, A. Scott, K. Daniell, K. Summerville, C. Price, S. Hudson, K. Kiakos, J. A. Hartley, T. Asao, M. Lee, *J. Med. Chem.* **2005**, *48*, 3903.

15 S. Nagamura, A. Asai, Y. Kanda, E. Kobayashi, K. Gomi, H. Saito, *Chem. Pharm. Bull.* **1996**, *44*, 1723.

16 Z.-F. Tao, I. Saito, H. Sugiyama, *J. Am. Chem. Soc.* **2000**, *122*, 1602.

17 K. Fujimoto, H. Iida, T. Bando, Z.-F. Tao, H. Sugiyama, *Nucleic Acids Res.* **2002**, *30*, 3748.

18 S. R. Rajski, R. M. Williams, *Chem. Rev.* **1998**, *98*, 2723.

19 a) T. Bando, H. Iida, I. Saito, H. Sugiyama, *J. Am. Chem. Soc.* **2001**, *123*, 5158. b) T. Bando, A. Narita, H. Sugiyama, *J. Am. Chem. Soc.* **2003**, *125*, 3471.

20 T. Bando, A. Narita, I. Saito, H. Sugiyama, *Chem. Eur. J.* **2002**, *8*, 4781.

21 a) D. L. Boger, T. Ishizaki, P. A. Kitos, O. Suntornwat, *J. Org. Chem.* **1990**, *55*, 5823. b) D. L. Boger, J. A. McKie, *J. Org. Chem.* **1995**, *60*, 1271.

22 T. Bando, A. Narita, K. Asada, H. Ayame, H. Sugiyama, *J. Am. Chem. Soc.* **2004**, *126*, 8948.

23 T. Bando, A. Narita, S. Sasaki, H. Sugiyama, *J. Am. Chem. Soc.* **2005**, *127*, 13890.

24 Z.-F. Tao, T. Fujiwara, I. Saito, H. Sugiyama, *Angew. Chem., Int. Ed.* **1999**, *38*, 650.

25 J. M. Belitsky, D. H. Nguyen, N. R. Wurtz, P. B. Dervan, *Bioorg. Med. Chem.* **2002**, *10*, 2767.

26 T. Bando, S. Sasaki, M. Minoshima, C. Dohno, K. Shinohara, A. Narita, H. Sugiyama, *Bioconjugate Chem.* **2006**, *17*, 715.

27 a) T. Oyoshi, W. Kawakami, A. Narita, T. Bando, H. Sugiyama, *J. Am. Chem. Soc.* **2003**, *125*, 4752. b) K. Shinohara, S. Sasaki, M. Minoshima, T. Bando, H. Sugiyama, *Nucleic Acids Res.* **2006**, *34*, 1189.

28 K. Shinohara, A. Narita, T. Oyoshi, T. Bando, H. Teraoka, H. Sugiyama, *J. Am. Chem. Soc.* **2004**, *126*, 5113.

29 T. Bando, H. Iida, Z.-F. Tao, A. Narita, N. Fukuda, T. Yamori, H. Sugiyama, *Chem. Biol.* **2003**, *10*, 751.

30 T. Bando, A. Narita, A. Iwai, K. Kihara, H. Sugiyama, *J. Am. Chem. Soc.* **2004**, *126*, 3406.

31 K. Shinohara, T. Bando, S. Sasaki, Y. Sakakibara, M. Minoshima, H. Sugiyama, *Cancer Sci.* **2006**, *97*, 219.

32 a) N. R. Cozzarelli, J. C. Wang, *DNA Topology and Its Biological Effects*, Cold Spring Harbor Laboratory Press, New York, **1990**. b) A. Travers, *Annu. Rev. Biochem.* **1989**, *58*, 427. c) A. H.-J. Wang, G. J. Quigley, F. J. Kolpak, J. L. Crawford, J. H. van Boom, G. A. van der Marel, A. Rich, *Nature* **1979**, *282*, 680.

33 a) R. R. Sinden, *DNA Structure and Function*, Academic Press, New York, **1994**. b) S. Niedle, *DNA Structure and Recognition*, IRL Press, Oxford, **1994**.

34 a) A. Herbert, A. Rich, *Proc. Natl. Acad. Sci. U.S.A.* **2001**, *98*, 12132. b) J. A. Hackett, D. M. Feldser, C. W. Greider, *Cell* **2001**, *106*, 275.

35 T. Schwartz, M. A. Rould, A. Herbert, A. Rich, *Science* **1999**, *284*, 1841.

36 T. Schwartz, J. Behlke, K. Lowenhaupt, U. Heinemann, A. Rich, *Nat. Struct. Biol.* **2001**, *8*, 761.

37 S. C. Ha, N. K. Lokanath, D. Van Quyen, C. A. Wu, K. Lowenhaupt, A. Rich, *Proc. Natl. Acad. Sci. U.S.A.* **2004**, *101*, 14367.

38 R. Liu, H. Liu, X. Chen, M. Kirby, P. O. Brown, K. Zhao, *Cell* **2001**, *106*, 309.

39 a) E. H. Blackburn, *Nature* **1991**, *350*, 569. b) J. L. Kim, D. B. Nikolov, S. K. Burley, *Nature* **1993**, *365*, 520. c) D. B. Nikolov, H. Chen, E. D. Halay, A. Hoffmann, R. G. Roeder, S. K. Burley, *Proc. Natl. Acad. Sci. U.S.A.* **1996**, *93*, 4862. d) Y. Kim, J. H. Geiger, S. Hahn, P. B. Sigler, *Nature* **1993**, *365*, 512. e) M. H. Werner, G. M. Clore, C. L. Fisher, R. J. Fisher, L. Trinh, J. Shiloach, A. M. Gronenborn, *Cell* **1995**, *83*, 761. f) M. A. Schumacher, K. Y. Choi, H. Zalkin, R. G. Brennan, *Science* **1994**, *266*, 763. g) M. H. Werner, J. R. Huth, A. M. Gronenborn, G. M. Clore, *Cell* **1995**, *81*, 705.

40 a) M. D. Shetlar, *Photochem. Photobiol. Rev.* **1980**, *5*, 105. b) F. Q. Hutchinson, *Rev. Biophys.* **1973**, *6*, 201.

41 a) H. Sugiyama, Y. Tsutsumi, I. Saito, *J. Am. Chem. Soc.* **1990**, *112*, 6720. b) H. Sugiyama, Y. Tsutsumi, K. Fujimoto, I. Saito, *J. Am. Chem. Soc.* **1993**, *115*, 4443.

42 H. Sugiyama, K. Fujimoto, I. Saito, E. Kawashima, T. Sekine, Y. Ishido, *Tetrahedron Lett.* **1996**, *37*, 1805.

43 H. Sugiyama, K. Fujimoto, I. Saito, *Tetrahedron Lett.* **1997**, *38*, 8057.

44 A. Rich, A. Nordheim, A. H.-J. Wang, *Annu. Rev. Biochem.* **1984**, *53*, 791.

45 H. Sugiyama, K. Kawai, A. Matsunaga, K. Fujimoto, I. Saito, H. Robinson, A. H.-J. Wang, *Nucleic Acids Res.* **1996**, *24*, 1272.

46 Y. Xu, R. Ikeda, H. Sugiyama, *J. Am. Chem. Soc.* **2003**, *125*, 13519.

47 K. Kawai, I. Saito, H. Sugiyama, *J. Am. Chem. Soc.* **1999**, *121*, 1391.

48 K. Kawai, I. Saito, E. Kawashima, Y. Ishido, H. Sugiyama, *Tetrahedron Lett.* **1999**, *40*, 2589.

49 T. Oyoshi, K. Kawai, H. Sugiyama, *J. Am. Chem. Soc.* **2003**, *125*, 1526.

50 Y.-G. Gao, S.-Y. Su, H. Robinson, S. Padmanabhan, L. Lim, B. S. McCrary, S. P. Edmondson, J. W. Shriver, A. H.-J. Wang, *Nat. Struct. Biol.* **1998**, *5*, 782.

51 T. Oyoshi, A. H.-J. Wang, H. Sugiyama, *J. Am. Chem. Soc.* **2002**, *124*, 2086.

52 a) W. I. Sunalquist, A. Klug, *Nature* **1989**, *342*, 825. b) D. Sen, W. Gilbert, *Nature* **1990**, *344*, 410. c) F. W. J. Smithfeigon, *Nature* **1992**, *356*, 164.

53 a) Y. Wang, D. J. Patel, *Biochemistry* **1992**, *31*, 8112.

b) M. P. Horvath, S. C. Schultz, *J. Mol. Biol.* **2001**, *310*, 367. c) C. Schaffitzel, I. Berger, J. Postberg, J. Hanes, H. J. Lipps, A. Plückthun, *Proc. Natl. Acad. Sci. U.S.A.* **2001**, *98*, 8572.
54 Y. Wang, D. J. Patel, *Structure* **1993**, *1*, 263.
55 G. N. Parkinson, M. P. Lee, S. Neidle, *Nature* **2002**, *417*, 876.
56 Y. Xu, Y. Noguchi, H. Sugiyama, *Bioorg. Med. Chem.* **2006**, *14*, 5584.
57 Y. Xu, H. Sugiyama, *J. Am. Chem. Soc.* **2004**, *126*, 6274.
58 F. Thoma, *EMBO J.* **1999**, *18*, 6585.
59 a) O. D. Schärer, *Angew. Chem., Int. Ed.* **2003**, *42*, 2946. b) D. O. Zharkov, G. Shoham, A. P. Grollman, *DNA Repair* **2003**, *2*, 839. c) S. Bjelland, E. Seeberg, *Mutat. Res.* **2003**, *531*, 37.
60 a) J. Cadet, T. Douki, D. Gasparutto, J. L. Ravanat, *Mutat. Res.* **2003**, *531*, 5. b) G. R. Martinez, A. P. M. Loureiro, S. A. Marques, S. Miyamoto, L. F. Yamaguchi, J. Onuki, E. A. Almeida, C. C. M. Garcia, L. F. Barbosa, M. H. G. Medeiros, P. D. Mascio, *Mutat. Res.* **2003**, *544*, 115.
61 S. Kawanishi, Y. Hiraku, S. Oikawa, *Mutat. Res.* **2001**, *488*, 65.
62 S. Steenken, S. V. Jovanovic, *J. Am. Chem. Soc.* **1997**, *119*, 617.
63 a) J. C. Fromme, A. Banerjee, S. J. Huang, G. L. Verdine, *Nature* **2004**, *427*, 652. b) H. Maki, M. Sekiguchi, *Nature* **1992**, *355*, 273. c) S. Shibutani, M. Takeshita, A. P. Grollman, *Nature* **1991**, *349*, 431. d) L. A. Lipscomb, M. E. Peek, M. L. Morningstar, S. M. Verghis, E. M. Miller, A. Rich, J. M. Essigmann, L. D. Williams, *Proc. Natl. Acad. Sci. U.S.A.* **1995**, *92*, 719. e) M. Moriya, *Proc. Natl. Acad. Sci. U.S.A.* **1993**, *90*, 1122. f) S. C. Baik, H. S. Youn, M. H. Chung, W. K. Lee, M. J. Cho, G. H. Ko, C. K. Park, H. Kasai, K. H. Rhee, *Cancer Res.* **1996**, *56*, 1279.
64 S. Matsugo, S. Kawanishi, K. Yamamoto, H. Sugiyama, T. Matsuura, I. Saito, *Angew. Chem., Int. Ed.* **1991**, *30*, 1351.
65 a) H. Sugiyama, I. Saito, *J. Am. Chem. Soc.* **1996**, *118*, 7063. b) I. Saito, M. Takayama, H. Sugiyama, K. Nakatani, A. Tsuchida, M. Yamamoto, *J. Am. Chem. Soc.* **1995**, *117*, 6406.
66 a) J. Cadet, M. Berger, G. W. Buchko, P. C. Joshi, S. Raoul, J.-L. Ravanat, *J. Am. Chem. Soc.* **1994**, *116*, 7403. b) K. Kino, I. Saito, H. Sugiyama, *J. Am. Chem. Soc.* **1998**, *120*, 7373.
67 W. Luo, J. G. Muller, C. J. Burrows, *Org. Lett.* **2001**, *3*, 2801.
68 F. Prat, K. N. Houk, C. S. Foote, *J. Am. Chem. Soc.* **1998**, *120*, 845.
69 J.-L. Ravanat, C. Saint-Pierre, J. Cadet, *J. Am. Chem. Soc.* **2003**, *125*, 2030.
70 H. Ikeda, I. Saito, *J. Am. Chem. Soc.* **1999**, *121*, 10836.
71 a) B. Giese, *Annu. Rev. Biochem.* **2002**, *71*, 51. b) K. Kawai, T. Majima, *J. Photochem. Photobiol., C* **2002**, *3*, 53. c) S. Delaney, J. K. Barton, *J. Org. Chem.* **2003**, *68*, 6475.
72 M. R. Arkin, E. D. A. Stemp, S. C. Pulver, J. K. Barton, *Chem. Biol.* **1997**, *4*, 389.
73 a) K. Kino, H. Sugiyama, *Chem. Biol.* **2001**, *8*, 369. b) K. Kino, H. Sugiyama, *Mutat. Res.* **2005**, *571*, 33.
74 T. Chen, G. P. Cook, A. T. Koppisch, M. M. Greenberg, *J. Am. Chem. Soc.* **2000**, *122*, 3861.
75 T. Ito, S. E. Rokita, *J. Am. Chem. Soc.* **2003**, *125*, 11480.
76 T. Watanabe, T. Bando, Y. Xu, R. Tashiro, H. Sugiyama, *J. Am. Chem. Soc.* **2005**, *127*, 44.
77 R. Tashiro, H. Sugiyama, *J. Am. Chem. Soc.* **2003**, *125*, 15282.
78 R. Tashiro, H. Sugiyama, *Angew. Chem., Int. Ed.* **2003**, *42*, 6018.
79 R. Tashiro, H. Sugiyama, *J. Am. Chem. Soc.* **2005**, *127*, 2094.
80 F. Thoma, *EMBO J.* **1999**, *18*, 6585.

Hiroshi Sugiyama was born in 1956 in Shizuoka, Japan, and received his Ph.D. from Kyoto University, Japan, in 1998 under the supervision of Prof. Teruo Matsuura. He was a Postdoctoral Fellow in Prof. Sidney Hecht's laboratory, University of Virginia, U.S.A., 1984–1986. He joined the Faculty of Engineering, Kyoto University, in 1987 and was promoted to an associate professor in 1993. He moved Tokyo Medical and Dental University (TMDU) as a full professor 1996 and has been a full professor in the Department of Chemistry, Graduate School of Science, Kyoto University since 2003. He received the Nippon IBM Award (1999) and The Chemical Society of Japan Award for Creative Work (2005).